502
7-17-84 JS(2)
DE+0212-7

Energy

GEOTHERMAL

DOE/NV/10150-4
(DE84011831)

BRINE AND GAS RECOVERY FROM GEOPRESSURED SYSTEMS: I. PARAMETRIC CALCULATIONS

Topical Report

By
S. K. Garg
T. D. Riney

February 1984

Work Performed Under Contract No. AC08-80NV10150

S-CUBED
La Jolla, California

Technical Information Center
Office of Scientific and Technical Information
United States Department of Energy

DISCLAIMER

This report was prepared as an account of work sponsored by an agency of the United States Government. Neither the United States Government nor any agency Thereof, nor any of their employees, makes any warranty, express or implied, or assumes any legal liability or responsibility for the accuracy, completeness, or usefulness of any information, apparatus, product, or process disclosed, or represents that its use would not infringe privately owned rights. Reference herein to any specific commercial product, process, or service by trade name, trademark, manufacturer, or otherwise does not necessarily constitute or imply its endorsement, recommendation, or favoring by the United States Government or any agency thereof. The views and opinions of authors expressed herein do not necessarily state or reflect those of the United States Government or any agency thereof.

DISCLAIMER

Portions of this document may be illegible in electronic image products. Images are produced from the best available original document.

DISCLAIMER

This report was prepared as an account of work sponsored by an agency of the United States Government. Neither the United States Government nor any agency thereof, nor any of their employees, makes any warranty, express or implied, or assumes any legal liability or responsibility for the accuracy, completeness, or usefulness of any information, apparatus, product, or process disclosed, or represents that its use would not infringe privately owned rights. Reference herein to any specific commercial product, process, or service by trade name, trademark, manufacturer, or otherwise does not necessarily constitute or imply its endorsement, recommendation, or favoring by the United States Government or any agency thereof. The views and opinions of authors expressed herein do not necessarily state or reflect those of the United States Government or any agency thereof.

This report has been reproduced directly from the best available copy.

Available from the National Technical Information Service, U. S. Department of Commerce, Springfield, Virginia 22161.

Price: Printed Copy A05
Microfiche A01

Codes are used for pricing all publications. The code is determined by the number of pages in the publication. Information pertaining to the pricing codes can be found in the current issues of the following publications, which are generally available in most libraries: *Energy Research Abstracts (ERA); Government Reports Announcements* and Index (*GRA* and I); *Scientific and Technical Abstract Reports (STAR);* and publication NTIS-PR-360 available from NTIS at the above address.

DOE/NV/10150-4
(DE84011831)
Distribution Category UC-66a

BRINE AND GAS RECOVERY FROM GEOPRESSURED SYSTEMS: I. PARAMETRIC CALCULATIONS

Topical Report

S. K. Garg and T. D. Riney

February 1984

Work Performed under Contract
DE-AC08-80-NV10150

Prepared for
Department of Energy
Nevada Operations Office

ABSTRACT

A series of parametric calculations was run with the S-CUBED geopressured-geothermal simulator MUSHRM to assess the effects of important formation, fluid and well parameters on brine and gas recovery from geopressured reservoir systems. The specific parameters considered are formation permeability, pore-fluid salinity, temperature and gas content, well radius and location with respect to reservoir boundaries, desired flow rate, and possible shale recharge. It was found that the total brine and gas recovered (as a fraction of the resource in situ) were most sensitive to formation permeability, pore-fluid gas content, and shale recharge.

TABLE OF CONTENTS

LIST OF TABLES

LIST OF FIGURES

LIST OF FIGURES (Continued)

I. INTRODUCTION AND BACKGROUND

1.1 Accessible Fluid-Resource Base

Many sedimentary basins contain formations with pore fluids at higher than hydrostatic pressures (vertical fluid-pressure gradients greater than about 0.465 psi/ft); these formations are termed "geopressured", and the energy contained in them is termed "geopressured-geothermal energy" (Wallace, et al., 1979). The geopressured strata are comprised of undercompacted clays and sandstones with the interstitial fluids bearing the bulk of the total overburden pressure. The fluid pressure is generally well in excess of hydrostatic. Further, these waters are hot and appear to be saturated with dissolved methane. Thus, the fluid contains energy in three forms; thermal energy, hydraulic (or pressure) energy, and chemical energy associated with the methane.

Among geopressured basins in the United States, the northern Gulf of Mexico basin has been most intensively investigated. During the past several years, several studies to define the magnitude of this resource base have been completed. Scientists of the United States Geological Survey (USGS) have published two assessments of the "accessible fluid resource base" (Papadopulous, et al., 1975 and Wallace, et al., 1979). The "accessible fluid resource base" is the fluid resource base at depths shallow enough to be reached by drilling in the forseeable future (Muffler and Cataldi, 1978). It should be noted that only a small fraction of the "accessible fluid resource base" may be economically recovered. Wallace, et al., (1979) used the term "geopressured-geothermal resources" to define the economically recoverable fraction. Wallace, et al., (1979) considered a surface area of 310,000 km^2 (~160,000 mi^2) for purposes of estimating the accessible fluid resource base in the

Cenozoic sedimentary formations beneath coastal Louisiana and Texas, the adjacent Gulf of Mexico continental shelf and in the inland Upper Cretaceous sandstone and shale. The depth of investigation was 6.86 km (~22,500 ft). Using information on subsurface fluid conditions from approximately 3500 wells, these authors estimated that the geopressured waters of the northern Gulf of Mexico basin contain 107,000 x 10^{18} J (~1.01 x 10^{20} Btu = 1.01 x 10^{5} quads) of thermal energy (referenced to 15°C ~ 59°F). Assuming that the geopressured waters are saturated with methane, the volume of methane dissolved in pore water was calculated to be 1670 x 10^{12} m^3 (~59,000 x 10^{12} ft^3). Of the nearly 196 x 10^{12} m^3 of geopressured brines in the northern Gulf of Mexico basin, approximately 10 percent of the fluid volume is in sandstones and the rest is in "shales". The sandstone reservoirs thus contain about 11,000 x 10^{18} J (~10^{19} Btu = 10^{4} quads) of thermal energy and 160 x 10^{12} m^3 (~5700 x 10^{12} ft^3) of methane. Thus, even if only a small fraction of the energy contained in the geopressured sandstones is economically recoverable, the geopressured zones would still represent a potentially enormous energy resource.

1.2 Recoverable Resource Base

The amount of fluid (brine and methane) producible from a geopressured reservoir by primary pressure depletion depends upon a number of formation and wellbore parameters. The most important of these parameters are; (1) reservoir volume (or drainage area and formation thickness), (2) formation (sandstone) porosity and permeability, (3) formation (sandstone) compressibility, (4) confining shale porosity, permeability and compressibility, (5) fluid pressure, temperature, salinity and methane content, and (6) wellbore (production) tubing diameter. The determination of almost all of these parameters requires the drilling and testing of wells. Since little or no well-test data were available prior to 1980 (see

Sec. 1.3 for a description of U.S. Department of Energy's well test program), the early (i.e., prior to 1980) recoverability studies were of necessity based upon assumed values for some of the critical reservoir parameters. In the following paragraphs, we briefly review several of these early recoverability investigations.

Papadopulous, et al., (1975) estimated the "accessible fluid resource base" to consist of 46,000 x 10^{18} J of thermal energy, 6.7 x 10^{14} m^3 of dissolved methane, and 200 x 10^{18} J of mechanical energy in both sandstones and shales in their study area (~145,000 km^2). They also estimated that (220-1500) 10^{18} J of thermal energy, (3.2-21.6) 10^{12} m^3 of dissolved methane, and (0-39) 10^{18} J of mechanical energy might be recoverable.

Jones (1976) estimated that 100,000 x 10^{12} ft^3 (~2800 x 10^{12} m^3) of methane were dissolved in geopressured waters (in sandstones and shales) in the northern Gulf of Mexico basin. He further concluded that 1146 x 10^{12} ft^3 (~32.5 x 10^{12} m^3) may be recoverable. Employing somewhat different assessment techniques, Hise (1976) estimated that only 3000 x 10^{12} ft^3 (85 x 10^{12} m^3) of methane was dissolved in the pore fluids of geopressured sandstones, and that 125 x 10^{12} ft^3 (~3.54 x 10^{12} m^3) was recoverable.

Hawkins (1977) considered the energy potential of Southern Louisiana, onshore and offshore to the outward limit of state-controlled waters. He concluded that 19.5 quads (20.6 x 10^{18} J) of thermal energy, 13.6 quads (14.3 x 10^{18} J ~ 3.83 x 10^{11} m^3) of methane energy and 1.2 quads (1.3 x 10^{18} J) of hydraulic energy might be producible.

Kuuskraa, et al., (1978) estimated the recoverable methane resource of onshore Texas and Louisiana to be 42 x 10^{12} ft^3

(~1.2 x 10^{12} m^3). They further suggested that the economically recoverable (at $3 per 1000 ft^3) resource was only 1.1 x 10^{12} ft^3 (~0.03 x 10^{12} m^3).

Wallace, et al. (1979), using the methodology of Papadopulous et al. (1975), estimated the recoverable resources in the northern Gulf of Mexico basin to be (270-2800) 10^{18} J of thermal energy and (4.2-44.0) 10^{12} m^3 of methane.

Swanson (1980) considered twenty specific onshore (surface area ~ 4000 sq. mi) geopressured fairways in Louisiana and Texas. The pore fluid (sandstone only) was estimated to contain 232 x 10^{12} ft^3 (~6.6 x 10^{12} m^3) of methane and 367 x 10^{15} Btu (~3.87 x 10^{20} J) of thermal energy. The maximum recoverable energy was predicted to be 7.6 x 10^{12} ft^3 (~0.22 x 10^{12} m^3) of methane and 12.6 x 10^{15} Btu (~1.33 x 10^{19} J) of thermal energy.

The National Petroleum Council (1980) study was restricted to seven specific Louisiana and four specific Texas onshore (total surface area ~ 454 sq. mi) geopressured prospects. These prospects were estimated to contain 6.7 x 10^{12} ft^3 (1.90 x 10^{11} m^3) of methane in place. The ultimate gas recovery (at a maximum gas price of $9 per 1000 ft^3 and a 10 percent Rate of Return) was predicted to be 568 x 10^9 ft^3 (1.61 x 10^{10} m^3).

As discussed by Wallace, et al. (1979), the various pre-1980 assessments cited above used different techniques and covered different areas. Therefore, the recovery figures presented are not directly comparable. As mentioned, a common weakness of all these studies was their reliance on estimated values for important reservoir parameters. Even though it is almost certain that only a very small portion of the accessible fluid resource base will be recoverable, more precise estimates of resource recovery will require some actual production data.

1.3 Department of Energy Well-Test Program

The U.S. Department of Energy (DOE) has the lead role in determining the technical, economic, and environmental feasibility of extracting energy from the geopressured resource. As part of it's geopressured program, DOE has been conducting a deep well drilling and testing program to help evaluate the resource. Four designed geopressured test wells have been drilled. Testing of these wells is, at present, in various stages of completion. In addition, several existing nonproductive petroleum and gas wells drilled into geopressured strata by private companies were re-entered and flow-tested under the DOE wells-of-opportunity (WOO) Program.

Basically, the "Design Wells" program was intended to test large (e.g., 1 cubic mile volume), potentially commercial geopressured reservoirs over extended time-periods. The "Wells of Opportunity (WOO)" program, on the other hand, was intended to secure fluid samples for determining fluid properties and dissolved gas content and to perform short-term production tests over a wider sample of geopressured reservoirs.

Petroleum and gas wells are commonly drilled-on-structure or near structural closure for hydrocarbon trapping. Thus, the wells of opportunity were usually unsuitable for testing large geopressured reservoirs. Testing of these wells, however, provided data on reservoir fluids (salinity, gas-water ratio, etc.) and formation characteristics around the wellbore. Selection criteria for Wells of Opportunity were enumerated by Westhusing (1981) and included the following:

1. Bottom-hole temperature greater than 275°F (flexible).
2. Pressure gradient of 0.8 psi/ft (flexible).

3. Salinity less than 75,000 mg/l TDS.

4. Minimum of 100 essentially continuous net feet of 100 percent water-saturated sandstone of good permeability, as determined by well log and core data.

5. Indication of adequate gas in solution.

The results from eight wells tested under the WOO program are summarized in Table 1. It is obvious from Table 1 that certain compromises had to be made in selecting the test wells. Five of the wells tested (Nos. 4 through 8) were bounded by one or more "sealing" faults/sand pinch-outs close to the wellbore. The temperature of the test wells ranged from a low of 234°F to a high of 327°F. Salinity values lie between 12,800 mg/L and 190,000 mg/L. The reservoir fluids in all cases appeared to be either close to saturation (with gas) or somewhat oversaturated; it is significant that several of the test wells produced a gas-water ratio in excess of the saturation value.

Selection of Design Well sites was based on research that attempted to identify localized areas where thick, high-pressure, high temperature sandstone masses existed as a result of isolation by growth faults, salt movement, facies boundaries or other factors. Design wells were intended to test large volume aquifers to ascertain whether geopressured reservoirs could be produced for extended periods at high flow rates. Testing of the wells was also expected to provide data on (1) formation permeability, (2) reservoir volume and fluid properties, (3) reservoir fluid (and possible sand) production, and (4) environmental factors such as brine disposal, surface subsidence and fault activation (Westhusing, 1981).

Table 1. Results from Wells of Opportunity Tested Under the Department of Energy's Geopressure Program

WELL (YEAR TESTED)	FORMATION	PRODUCING INTERVAL DEPTH, FT	GROSS (NET) SAND THICKNESS (FT)	RESERVOIR PRESSURE PSIA	TEMPERATURE (^{o}F)	SALINITY TDS (MG/L)	LABORATORY GAS/WATER SOLUTION RATIO SCF/BBL	POROSITY (%) PERMEABILITY (MD)	MAXIMUM, FLOW RATE BBL/DAY	PRODUCING GAS/WATER RATIO SCF/BBL	RESERVOIR DESCRIPTION AND COMMENTS
1. COASTAL STATES EDNA DELCAMBRE NO.1(1977) [1]	PLANULINA ZONE (SAND 1)	12,573-12,605	(30)	10,858	234	134,600	21.0*	29 100-364	11,958	20-62	GAS-ZONE NEAR WELL?
	MIOCENE (SAND 3)	12,869-12,911 (PERFORATED INTERVAL)	(~48)	11,012	238	114,100	19.8* *SEPARATOR-GAS	26 447	8,732	48-86	
2. NEUHOFF OIL CO. FAIRFOX FOSTER SUTTER NO.2 WELL(1979) [2]	MA-6 LOWER MIOCENE	15,781-15,916	135 (58)	12,220	270	190,904	±22.8	19 ~14	~7,700	±22.8	WELL BETWEEN TWO PARALLEL FAULTS (FAULT SEPARATION ~1900 FT)
3. SOUTHPORT EXPLORATION BEULAH SIMON NO.2 (1979) [3]	CAMERINA (UPPER OLIGOCENE)	14,674-14,770 (PERFORATED INTERVAL)	208 (186)	13,015	266	103,925	±24.0	19 ~12	~11,000	±24.0	TWO PARALLEL FAULTS AT ~556 FT AND ~794 FT FROM WELL
4. WAINOCO OIL & GAS CO., P.R. GIROUARD NO.1(1980) [4]	FRIO-MARG. TEX NO. 1 MIDDLE OLIGOCENE	14,744-14,819 (PERFORATED INTERVAL)	107 (91)	13,203	274	23,400	44.5	±26 200-240	15,000	40	LENTICULAR ZONE WITH A FLOW ANGLE <50 DEG.
5. LEAR PETROLEUM EXPLORATION KOELEMAY NO.1(1980) [4]	YEGUA- "LEGER" MIDDLE EOCENE	11,639-11,780	139 (77)	9,450	260	15,000	35	~26 100-200	3,200	30-318* *WELL PRODUCING GAS AND OIL AT TEST COMPLETION.	LENTICULAR, SAND WITH VERY RESTRICTED FLOW AREA. UPDIP ATTIC HYDROCARBON SATURATED ZONE.
6. RIDDLE OIL CO. SALDANA NO.2(1980) [4]	UPPER WILCOX UPPER EOCENE	9,745-9,820 (PERFORATED ZONE)	90 (79)	6,627	300	12,800	41	20 16.7	1,950	47-54	TWO BARRIERS WITHIN 265 FT OF WELLBORE. FLOW ANGLE <111 DEG.

Table 1. Results from Wells of Opportunity Tested Under the Department of Energy's Geopressure Program (Continued)

	WELL (YEAR TESTED)	FORMATION	PRODUCING INTERVAL DEPTH, FT	GROSS (NET) SAND THICKNESS (FT)	RESERVOIR PRESSURE PSIA	TEMPERATURE (^{o}F)	SALINITY TDS (MG/L)	LABORATORY GAS/WATER SOLUTION RATIO SCF/BBL	POROSITY (%) PERMEABILITY (MD)	MAXIMUM FLOW RATE BBL/DAY	PRODUCING GAS/WATER RATIO SCF/BBL	RESERVOIR DESCRIPTION AND COMMENTS
7.	HOUSTON OIL & MINERALS, PRAIRIE CANAL NO.1(1981) [4]	HACKBERRY UPPER FRIO	14,782-14,820	25 (14)	12,942	294	42,600	43	25 95	7,100	43-55	CLOSE-IN SAND PINCH-OUT AND/OR FAULTS. FLOW ANGLE <40 DEG.
8.	MARTIN EXPLORATION, CROWN ZELLERBACH NO.2(1981) [4]	TUSCALOOSA UPPER CRETACEOUS	16,720-16,750 (PERFORATED ZONE)	36 (35)	10,075	327	32,000	UNAVAILABLE	±17 16.6	2,832	33	AT LEAST ONE BARRIER ABOUT 142 FT FROM WELLBORE.

[1] DATA ABSTRACTED FROM PROCEEDINGS OF 3RD AND 4TH GEOPRESSURED-GEOTHERMAL ENERGY CONFERENCES.

[2] DATA ABSTRACTED FROM WILLITS, M.H., R.L. MCCOY, R.J. DOBSON AND J.H. HARTSOCK, "INVESTIGATION AND EVALUATION OF GEOPRESSURED-GEOTHERMAL WELLS, FINAL REPORT- FAIRFAX FOSTER SUTTER NO. 2 WELL, ST. MARY PARISH, LOUISIANA," DOE REPORT NO. DOE/ET/28460-1, DECEMBER 1979.

[3] DATA ABSTRACTED FROM DOBSON, R.J., J.H. HARTSOCK, R.L. MCCOY AND J.A. RODGERS, "INVESTIGATION AND EVALUATION OF GEOPRESSURED-GEOTHERMAL WELLS, FINAL REPORT- BEULAH SIMON NO. 2 WELL, VERMILION PARISH, LOUISIANA," DOE REPORT NO. DOE/ET/28460-3, JULY 1980.

[4] DATA ABSTRACTED FROM KLAUZINSKI, R.Z., "TESTING OF SIX 'WELLS OF OPPORTUNITY' DURING PERIOD 1980 AND 1981," PROCEEDINGS 5TH CONFERENCE GEOPRESSURED-GEOTHERMAL ENERGY, BATON ROUGE, LOUISIANA, PP. 171-176, OCTOBER 1981.

Table 2. Results from Design Wells Tested Under the Department of Energy's Geopressure Program (Status as of March 1983)

	WELL (YEAR TESTED)	FORMATION	PRODUCING INTERVAL DEPTH, FT	GROSS (NET) SAND THICKNESS (FT)	RESERVOIR PRESSURE PSIA	TEMPERATURE (^{o}F)	SALINITY TDS (MG/L)	LABORATORY GAS/WATER SOLUTION RATIO SCF/BBL	POROSITY (%) PERMEABILITY (MD)	MAXIMUM FLOW RATE BBL/DAY	PRODUCING GAS/WATER RATIO SCF/BBL	RESERVOIR DESCRIPTION AND COMMENTS
1.	PLEASANT BAYOU NO.2 (1979,1980) [1]	FRIO OLIGOCENE	14,644-14,704	(60)	~11,168	~306	~130,000	~27* *FROM CORRELATIONS	~17.6 ~192	~19,000	~23* *SEPARATOR VALUE (800 PSIA)	ONE BARRIER AT ~3000 FT FROM WELLBORE. RESERVOIR VOLUME ~0.4 MI^{3}.
2.	MG-T/DOE AMOCO FEE NO. 1 WELL (1981) [2]	MIOGYP SAND FRIO UPPER OLIGOCENE	15,387-15,414	(27)	~12,082	~299	~165,000	~34* *RECOMBINATION MEASUREMENT (WEATHERLY LABORATORIES) ~24** **CORRELATIONS	22 162 FOR R ≤ 200 FT; ~12 FOR R ≥ 200 FT	~16,000	23-27	TWO ALTERNATIVE RESERVOIR INTERPRETATIONS: (1) LOW PERMEABILITY BEYOND 200 FT (2) FLOW ANGLE ~26 DEG.
3.	DOW-DOE SWEEZY NO.1 WELL (1981-1982) [3]	UPPER FRIO OLIGOCENE	13,349-13,388 13,395-13,406	(50)	~11,410-11,447	~237	~100,900	UNAVAILABLE	27 133	~11,000	±20	RESERVOIR AREA ~830 ACRES. SOME EVIDENCE OF RECHARGE

[1] GARG, S.K., T.D. RINEY AND J.M. FWU, "ANALYSIS OF PHASE I FLOW DATA FROM PLEASANT BAYOU NO 2 GEOPRESSURED WELL," PROCEEDINGS 5TH CONFERENCE GEOPRESSURED-GEOTHERMAL ENERGY, BATON ROUGE, LOUISIANA, PP. 97-100, OCTOBER 1981.

[2] GARG, S.K., "ANALYSIS OF FLOW DATA FROM THE MG-T/DOE AMOCO FEE NO. 1 WELL," DOE REPORT NO. DOE/NV/10150-3 JANUARY 1982.

[3] DATA ABSTRACTED FROM PRESENTATIONS BY J. HAMILTON AND S.K. GARG AT THE DOE/INDUSTRY GEOPRESSURED GEOTHERMAL RESOURCE DEVELOPMENT PROGRAM WORKING GROUP MEETINGS, HOUSTON, TEXAS, DECEMBER 1982.

Under the design wells program, the following four wells were drilled:

1. Fenix and Scisson, Pleasant Bayou No. 2 Well, Brazoria County, Texas.

2. Magma Gulf-Technadril-DOE, Amoco Fee No. 1 Well, Sweet Lake Field, Cameron Parish, Louisiana.

3. Dow-DOE, L. R. Sweezy No. 1 Well, Parcperdue Field, Vermilion Parish, Louisiana.

4. Technadril-Fenix and Scisson-DOE, Gladys McCall No. 1 Well, Cameron Parish, Louisiana.

Testing of the Sweezy No. 1 well is now complete. Preliminary short term and Phase I (45 days production) testing of Pleasant Bayou No. 2 was performed during 1979 and 1980; this well was recently flowed at a more or less constant rate (~20,000 BPD) to establish the long-term production characteristics. An Initial Flow Test (~3 days) and a Reservoir Determination Test (~17 days) were completed on the Amoco Fee No. 1 well in 1981; this well was then shut-in until recently due to funding problems. Testing of the Gladys McCall well is in progress.

Table 2 summarizes the results available from three of the Design Wells (reservoir description and permeability data are taken from analyses performed by S-CUBED). The pore fluids from two wells (Pleasant Bayou and Sweezy) are close to saturation; the Amoco Fee reservoir, on the other hand, appears to be undersaturated with respect to dissolved gas. Reservoir temperatures vary from a low of 237°F (Sweezy well) to a high of 306°F (Pleasant Bayou). Fluid salinities lie in the range 100,900 mg/L to 165,000 mg/L. The Pleasant Bayou No. 2 well produced from a reservoir of fairly large

volume (more than 0.4 mi^3). Apart from a fault-boundary at 3000 ft from the well, no other boundaries were encountered during the 45-day Phase I test. The formation permeability for the Pleasant Bayou well was also relatively high. The Dow-DOE L. R. Sweezy No. 1 well was designed to deplete a reservoir of limited volume. The reservoir area obtained from an analysis of well-test data (~830 acres) was in reasonable agreement with that given by geology study (~940 acres). It does, however, appear that the formation in the Sweezy area is much more compressible than that in the Pleasant Bayou area. In addition, there exists some evidence of fluid recharge (shale dewatering and/or leaky boundary) in this (Sweezy) reservoir. The Amoco Fee No. 1 well exhibited a much larger than anticipated pressure-drawdown during flow-testing. Analysis of downhole pressure data indicates that the Amoco Fee No. 1 well penetrated a zone of relatively high permeability; this high permeability zone, however, extends to a radius of only 200 ft from the well. The far-field permeability (i.e., for $r > 200$ ft) appears to be rather low. No other reservoir boundaries/mobility changes can be identified from the test data. An alternate interpetation of the test data for Amoco Fee No. 1 well would be to assume that the flow to the well is severely restricted by the presence of two intersecting faults (graben angle ~ 26˚) located at about 200-250 ft from the well.

1.4 Recoverable Resource and Study Design

The DOE well test program has yielded a wealth of information regarding geopressured pore-fluid and formation properties. The principal purpose of this report is to use these data to assess energy recovery from relatively large volume geopressured reservoirs.

Although the available data (from the DOE well-test program) are sufficiently comprehensive, as far as reservoir fluid properties

and formation porosities and permeabilities are concerned, this is not the case in regard to reservoir volume and formation compressibility (only limited amount of data from three design wells are available to define these parameters). In this connection, it should be noted that the maximum volume of fluid producible from a geopressured reservoir by primary pressure depletion is equal to $VC_T (P_i - P_h - P_f)$, where

V	=	reservoir volume
C_T	=	total formation compressibility (= $[1-\phi]/\phi \ C_m + C_f$)
$C_m(C_f)$	=	uniaxial formation (fluid) compressibility
ϕ	=	formation porosity
P_i	=	initial reservoir pressure
P_h	=	hydrostatic pressure, and
P_f	=	frictional pressure drop in the production tubing

It is currently impractical to define recoverable resource on the basis of productivity calculations for well-defined geopressured reservoirs, because of the unavailability of relevant data from a sufficient number of large volume geopressured reservoirs.

Therefore, it was decided to conduct this study in two parts. In this first part of the study, we adopt the Pleasant Bayou reservoir as the base case. The various formation (with the exception of compressibility and reservoir volume), fluid and wellbore properties are then varied around their base values to assess their impact on energy recovery. The specific parameters considered are formation permeability, pore-fluid salinity, temperature and gas content, well radius and location with respect to boundaries, desired flow rate, and possible shale recharge. These calculations are discusssed in detail in Section II of this report. The second part of this study is planned to evaluate energy recovery from specific geopressured reservoir systems. These two studies,

taken together, will hopefully provide a more realistic perspective on energy recovery from geopressured systems than that available from existing assessments.

II. PARAMETRIC STUDIES

2.1 Pleasant Bayou Reservoir

Selection of the sites for the Design Wells was based on research that attempted to identify large volume, high pressure and high temperature geopressured reservoirs. From an analysis of available data, University of Texas researchers identified five "Geothermal Fairways" - Hidalgo, Armstrong, Corpus Christi, Matagorda and Brazoria - in the Frio formation along the Texas Gulf Coast that appear to have thick sandstone bodies with high temperatures. Of these fairways, the Brazoria fairway in Brazoria County appeared to be most promising and the Pleasant Bayou prospect was developed within this fairway. A detailed description of the geology of the prospect area is given by Bebout, et al., (1979) and Loucks, et al., (1979).

The first well drilled at the Pleasant Bayou site (Pleasant Bayou No. 1, drilled in 1978) is being used for waste brine reinjection since well completion problems precluded its use for geopressured reservoir testing. A second well (Pleasant Bayou No. 2) was drilled in 1979 in the immediate vicinity of the first to obtain the transient flow data needed to evaluate geopressured reservoir behavior. The test well penetrated several potentially productive sands; however, to date, only sand C (depth interval 14,644 ft - 14,704 ft, net sand thickness = 60 ft) has been flow-tested. The Pleasant Bayou No. 2 well was completed with 7 inch perforated casing set through the Frio sand at 14,644 ft to 14,704 ft. The production is through a 5-1/2 inch tubing.

A series of five preliminary short-term (times ranging from 13 minutes to 10.5 days) production and buildup tests of the Pleasant Bayou No. 2 well were performed during the second half of 1979.

Phase I of the long-term testing of this well (~45 days production, ~45 days shutin) was conducted from September 16 to December 15, 1980. Bottomhole pressure was measured using the Hewlett-Packard quartz crystal element. Turbine pulse meters, downstream of the separator, were employed to record brine flow rates. Gas flow rates, however, were indirectly calculated. Analysis of pressure drawdown/buildup data from the Phase I test (see Garg, et al., 1981) indicated (1) the presence of a linear barrier at approximately 3000 ft from the well, and (2) that the skin factor increases more or less linearly with the flow rate. The linear barrier appears to correspond to a mapped growth fault. Based upon buildup pressures extrapolated to infinite time, the reservoir volume is calculated to be of the order of 0.4 mi^3. The other important formation and fluid properties derived from analysis of the data are as follows:

Formation Porosity, ϕ: 0.176
Formation Permeability, k: 192 md
Initial Reservoir Pressure, P_i (14,674 ft depth): 11,168 psi
Reservoir Temperature: 306°F
Salinity: 130,000 mg/l (~0.12 gm of salt/gm of brine)
Fluid Compressibility, C_f: 3×10^{-6} psi^{-1}
Uniaxial Formation Compressibility, C_m: 10^{-6} psi^{-1}
Total Formation Compressibility, C_T ($= [1-\phi]/\phi\, C_m + C_f$): 7.7×10^{-6} psi^{-1}

With temperature T = 306°F, p_i = 11,168 psi and salinity s ≈ 0.12 gm/gm, the methane-brine equation-of-state data (Pritchett, et al., 1979) yield a methane concentration of 27.2 standard cubic feet per stock tank barrel (SCF/STB) at saturation. The Gas Water Ratio (GWR) during Phase I flow tests averaged around 23 SCF/STB at separator conditions; this suggests that the reservoir fluids are most probably saturated with gas.

2.2 The MUSHRM Reservoir Simulator

Numerical reservoir simulation ordinarily involves subdividing the region of interest (i.e., the reservoir) into a grid of discrete zones or "blocks", and then solving for the flow in a time-marching fashion using finite-difference analogues of the principles of mass, momentum, energy and species conservation. Given properly posed initial and boundary conditions and constitutive descriptions of the formation rock and the fluid mixture inhabiting the pores, solutions may be obtained which consist, at each time step, of descriptions of "average" conditions prevailing in each of the blocks which make up the computational grid. In such a reservoir description, the flow may be multicomponent (several fluid species), multiphase (liquid, gas and pore solids), unsteady and non-isothermal.

For many applications, such as numerical simulationn of well testing or resource recoverability, it is desirable to predict, as a function of time, conditions (particularly the pressure) at the sand-face of a production well within such a reservoir. A numerical simulator such as the one described above is capable of predicting well-block conditions at each time step (the well-block is the computational zone in which the well is located), but these conditions are not generally the same as sand-face conditions since the well-block is normally much larger in size than the wellbore diameter.

The geothermal-geopressured simulator (MUSHRM) employed in this study treats the flow of the fluid in the vicinity of a production (or injection) well by incorporating a well-bore "sub-grid model" (Pritchett, et al, 1979). The well-bore "sub-grid model" assumes that the fluid flow between the "equivalent well-block radius" and the sand-face can be treated as steady over the time step employed. Numerical experimentation with this model has shown that "steady-state assumption" is adequate for treating

such effects as increase of free-gas saturation near the sand-face due to decreasing pressure. The subgrid model is valid for non-isothermal flow and includes treatment of a well that penetrates more than one grid block, as is often the case in axisymmetric and three-dimensional finite-difference grid configurations. A detailed description of the sub-grid model and the techniques developed for its incorporation into the MUSHRM simulator have been given in the earlier report (Pritchett, et al, 1979).

The MUSHRM simulator in its present form is a rather general program for treating the important mechanisms in geopressured-geothermal systems. MUSHRM can treat one-dimensional slab, cylindrical or spherical, two-dimensional plane or axisymmetric, and three dimensional cartesian geometries. Each computational block may contain a different rock type; a rock type is characterized by (1) density and porosity, (2) directional absolute permeabilities, (3) relative permeability function, (4) heat capacity and thermal conductivity, (5) porosity-pore pressure and temperature relation, and (6) permeability-porosity relation. A rather comprehensive fluid constitutive package for brine/methane mixtures is employed for geopressured-geothermal MUSHRM simulations. Provision is made for all practical boundary conditions, and for any face of any computational block to be a boundary. The user may specify distributed internal fluid mass or heat sources/sinks within the computational grid. For each well, the user may impose production/injection rates or sand-face pressures at some depth.

MUSHRM does not simulate chemical interactions that might occur in the reservoir as the pressure and temperature conditions are changed from their initial in situ equilibrium values. The temperature change, however, was calculated to be less than 1°F for each of the cases considered in this study. Precipitation of minerals from the brine in the vicinity of the sandface due to

pressure drawdown has not been a problem in tests made on geopressured wells (Tomson, M., personal communication, February 1984). Scaling and corrosion within the production wellbore are serious engineering problems but are not of concern here. Further, precipitation of minerals in the cooled and depressureized waste fluid, and chemical interactions between it and sandface formation rock, can lead to plugging of injection wells. A specialized computer model to simulate the combined physicochemical processes which occur in the vicinity of an injection well for spent geopressured brine is described elsewhere (Alexander, et al, 1981).

2.3 Base Case

For simulation purposes, the reservoir was assumed to be a rectangular volume with the following dimensions:

Length, L = 42,000 ft
Width, w = 24,000 ft
Height, h = 60 ft
Volume, V = Lwh = 6.048×10^{10} ft^3 ≈ 0.41 mi^3

A two-dimensional areal representation of the reservoir along with the numerical grid (8 x 9) is shown in Figure 1. The production well is located 3000 ft from the bottom boundary. Note that because of symmetry in the x-direction (or i), it is only necessary to consider the left (or right) half of the reservoir. (In this case, it is of course necessary to divide the true well production rate by two so that the proper amount of fluid will be withdrawn per unit time from the reduced grid volume. Furthermore to obtain the proper pressure drop between the "effective wellblock radius" r_o and the well sandface, it is essential that the value of the open interval for the well be reduced by the same factor. Also, the effective wellbore radius r_o is defined somewhat differently. With these changes, the calculated wellbore pressure history should be the same as if the entire region had been considered. To avoid confusion, we

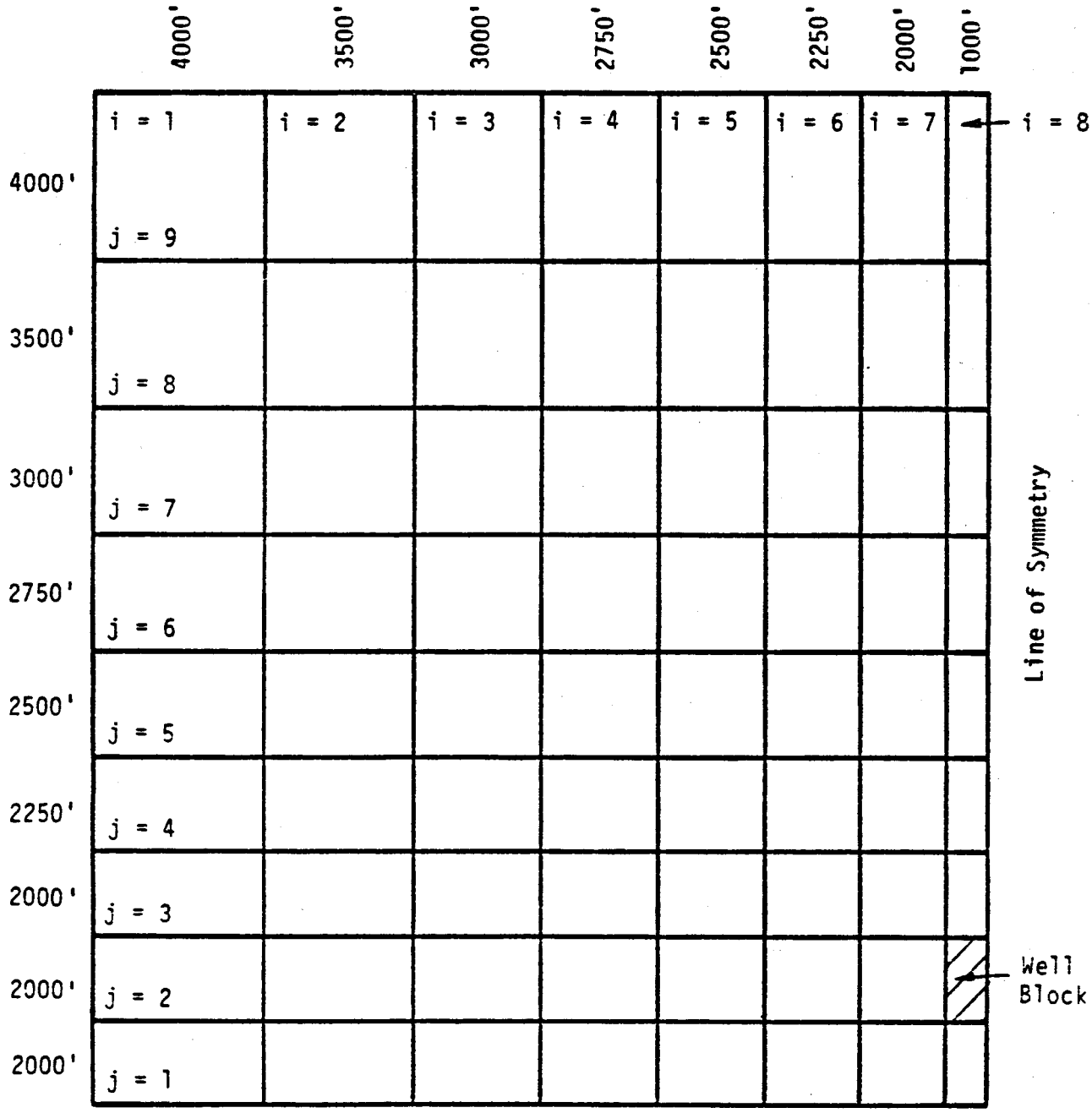

Figure 1. An Areal Cross-Section of the Reservoir. All boundaries are impermeable and insulated. The reservoir cross-section (left half) is represented by an 8 x 9 rectangular mesh. The production well is assumed to be located at the geometric center of the production grid block.

shall in the following, give only the true well production rate and the true open interval for the wellbore.)

The reservoir formation is assumed to be a sandstone with the following properties.

Initial porosity, $\phi_0 = 0.18$

Grain density, $\rho_r = 164.4$ lbm/ft^3 ($\simeq 2.633 \times 10^3$ kg/m^3)

Grain specific heat, $c_{vr} = 0.23$ Btu/lbm°F ($\simeq 0.963$ kJ/kg°C)

Initial permeability, $k_0 = 190$ md ($\simeq 190 \times 10^{-15}$ m^2)

Grain thermal conductivity, $K_r = 3.03$ Btu/hr-ft°F ($\simeq 5.25$ W/m°C)

Uniaxial compressibility, $C_m = 10^{-6}$ psi^{-1} ($\simeq 0.145 \times 10^{-9}$ Pa^{-1})

Pleasant Bayou No. 2 well displays a variable skin which increases more or less linearly with flow rate. For purposes of this simulation, the skin factor is considered to be zero. This is justified in view of the fact that the principal goal of this work is to assess the productivity of geopressured reservoirs using reasonable formation and pore fluid parameters; the use of a nonzero skin (which will presumably change from well to well) will only introduce additional complications.

Laboratory measurements (Roberts, 1980) of relative permeabilities on several cores obtained from the two Pleasant Bayou wells show that the liquid phase relative permeability declines with small amounts of free gas in the pores. Sufficient data are, however, unavailable to characterize the liquid relative permeability decline at low free gas saturations ($S_g < 5$ percent). In the absence of data, the relative permeability curves used are those of Martin (1979) (see Figure 2). The residual gas saturation (S_{gr}) is taken to be 5 percent; S_{gr} is one of the most important parameters governing the production of methane from geopressured aquifers. Even though the exact value of S_{gr} for geopressured aquifers is unknown, the experience from oil and gas

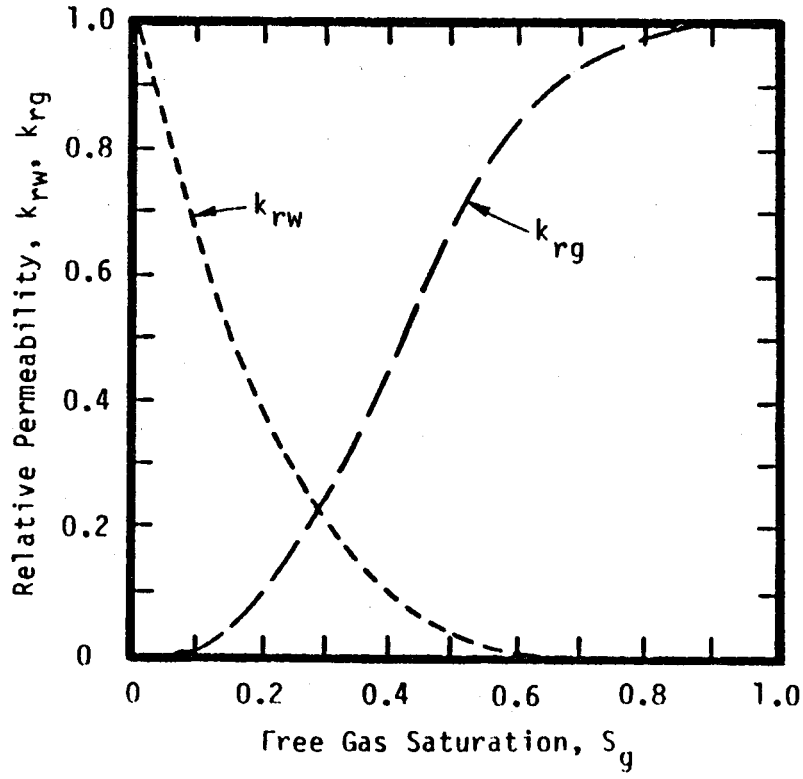

Figure 2. Relative Permeability Curves Used in Simulations (Martin, 1979)

reservoirs suggests that it may be at least 2 to 5 percent (Doscher, et al., 1982). The numerical simulations of both Martin (1979) and Doscher, et al., (1982) imply that for initial free gas saturations significantly less than S_{gr}, the produced gas-water ratio (GWR) will be less than its (GWR) value at saturation.

A drop in pore pressure causes a reduction in porosity ϕ and permeability k. The instantaneous porosity ϕ and permeability k are given by the following equations:

$$\frac{\partial \phi}{\partial t} = (1 - \phi)\, C_m \frac{\partial p}{\partial t}$$

$$k = k_o \left(\frac{\phi}{\phi_o}\right)^3 \left(\frac{1 - \phi_o}{1 - \phi}\right)^2 ,$$

where p = fluid pressure

t = time.

The reservoir fluid is a methane saturated brine with salinity by mass of S = 0.12 (this corresponds to a dissolved solids content of approximately 130,000 mg/L at standard conditions). The standard conditions, in conformity with general practice in petroleum industry, are taken to be P = 14.7 psi and T = 60°F. The initial pore pressure, temperature and methane mass fraction at a depth of 14,674 ft (middle of perforated interval) are p = 11,168 psi (≈ 770 x 10^5 Pa), T = 306°F (≈ 152.2°C), and C = 0.003018*. The amount of methane dissolved in brine at reservoir conditions is approximately 27.2 SCF/STB. The reservoir fluid flows from the formation into a single fully-penetrating 7-inch diameter well.

*The density of methane-saturated brine at reservoir conditions is 1035.5 kg/m^3 (≈ 164.6 kg/bbl). Also, the density of brine at standard conditions is 1087 kg/m^3 (≈ 172.8 kg/STB). This yields a formation volume factor B of 172.8/164.6 ≈ 1.050 reservoir bbl/STB. The viscosity of brine at reservoir conditions is 0.267 cp. Furthermore, the specific volume of methane at standard conditions is taken to be 52.0 SCF/kg.

The well is produced at a constant rate of 40,000 STB/D (≈ 80.24 kg/s) until the bottom-hole pressure p_{wf} (at datum 14,674 ft) falls to 7250 psi* (≈ 500 x 10^5 Pa). Thereafter, the bottom-hole pressure is maintained at 7250 psi and fluid production is allowed to decline. The production from a geopressured well will decline to zero when the fraction of total fluid produced is $C_T (P_i - P_h - P_f)$. With P_i = 11,168 psi, an average $(P_h + P_f)$ of 7,250 psi, and a C_T of 7.56 x 10^{-6} psi^{-1}, the fraction of reservoir fluid producible by pressure depletion is approximately 3.0 percent. The latter figure represents an upper limit (in the absence of recharge) of the producible resource since declining flow rate will cause abandonment of a well before the production rate reaches zero. In the present series of calculations, production is terminated when the methane production rate falls below 100,000 SCF/D, or when the production time exceeds thirty years.

2.4 Formation Permeability

Formation permeability is one of the most important production parameters. Swanson (1980) estimated formation permeabilities in the range (1-10) md. Results from the DOE well-testing programs, however,

*Assuming a hydrostatic gradient of 0.46 psi/ft, the hydrostatic head is 0.46 (14,674) ≈ 6750 psi. Thus, minimum bottom-hole pressure is set at hydrostatic head plus 500 psi. It is implicitly assumed here that two-phase flow occurs in the wellbore, and that sufficient gas percolates through the liquid column to reduce P_h, such that $(P_h + P_f) < 7,250$ psi, where P_f denotes the frictional pres- sure drop in the production tubing. Since the frictional pressure drop will vary with the flow rate, the minimum bottom-hole pressure will depend somewhat on the flow rate. However, for purposes of these calculations, it is sufficient to assume a constant minimum bottom-hole pressure. At any rate, for flow rates less than 10,000 STB/D, the total pressure loss $(P_h + P_f)$ in the Pleasant Bayou No. 2 well is of the order of 6700 psi.

suggest the existence of many discrete geopressured intervals with permeablities lying between 10 md and 300 md. To show the sensitivity of production to formation permeability, calculations were run for three values of permeability (20 md, 100 md, and the base case of 190 md). Results of these calculations are shown in Figures 3, 4 and 5, and in Table 3.

For k = 20 md, it is impossible to maintain the desired production rate of 40,000 bbl/D for an extended period of time. As a matter of fact, the initial production rate is only slightly over 10,000 bbl/D. With larger formation permeabilities, the production rate of 40,000 bbl/D can be sustained for a short period of time after which the rate begins to decline. It is apparent from Figures 4 and 5 that with a decrease in formation permeability, it takes longer to produce the reservoir. The cumulative production of brine and methane are essentially the same for both k = 100 md and k = 190 md. With k = 20 md, it is possible to produce only about one-half of the theoretically producible reservoir fluid. Figure 3 shows that bottom-hole pressure falls to its minimum value in less than 2 1/2 years for k = 190 md. This implies that it would be extremely difficult to recover any useful hydraulic energy from geopressured systems. Finally, Table 3 indicates that the average produced GWR is less than 90 percent of the GWR at saturation. This is attributed to gas evolving from solution with pore pressure drop. The evolved gas will remain in the formation until the free gas volume in the pores exceeds the residual gas saturation value. Even if all the gas is liberated within the reservoir (starting from 11,168 psi down to 7,250 psi), the resulting gas saturation in the formation pores will be an order of magnitude less than the residual gas saturation of 5 percent.

2.5 Gas Content

The produced gas-water ratios from geopressured wells tested so far span quite a large range, indicating that while some geopressured reservoirs are close to saturation, others may be either

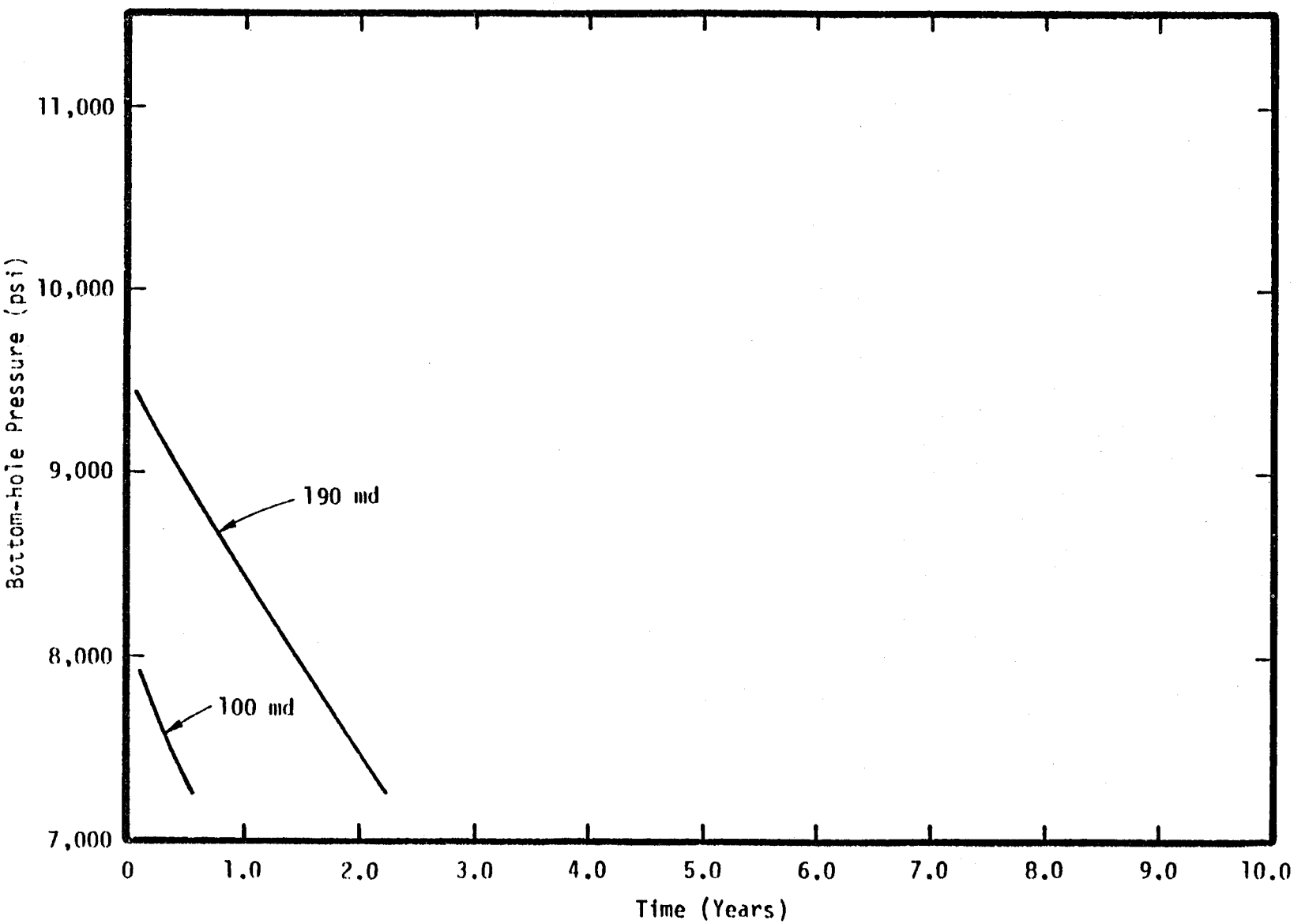

Figure 3. Effect of Formation Permeability on Bottom-hole Pressure

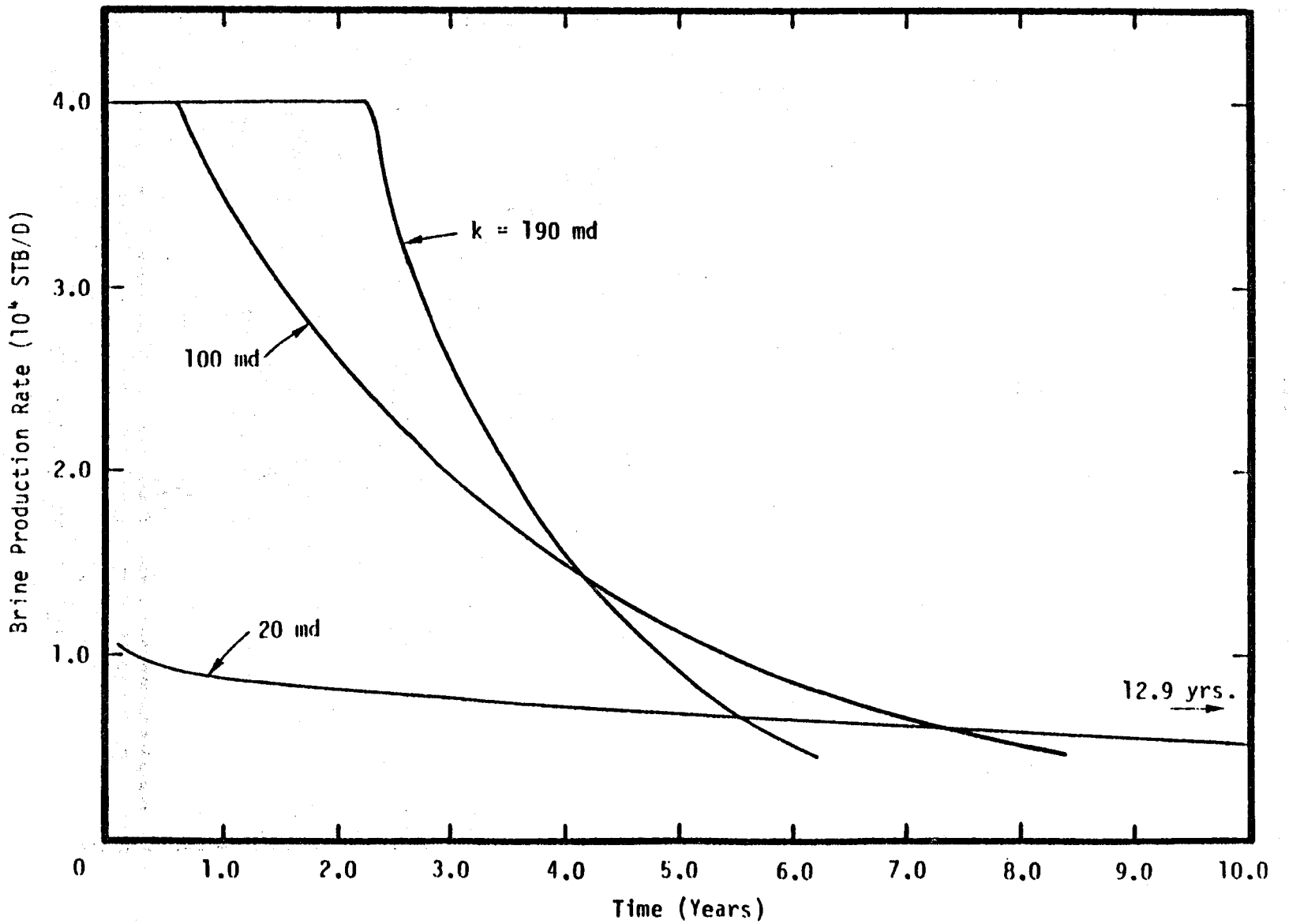

Figure 4. Effect of Formation Permeability on Brine Production Rate

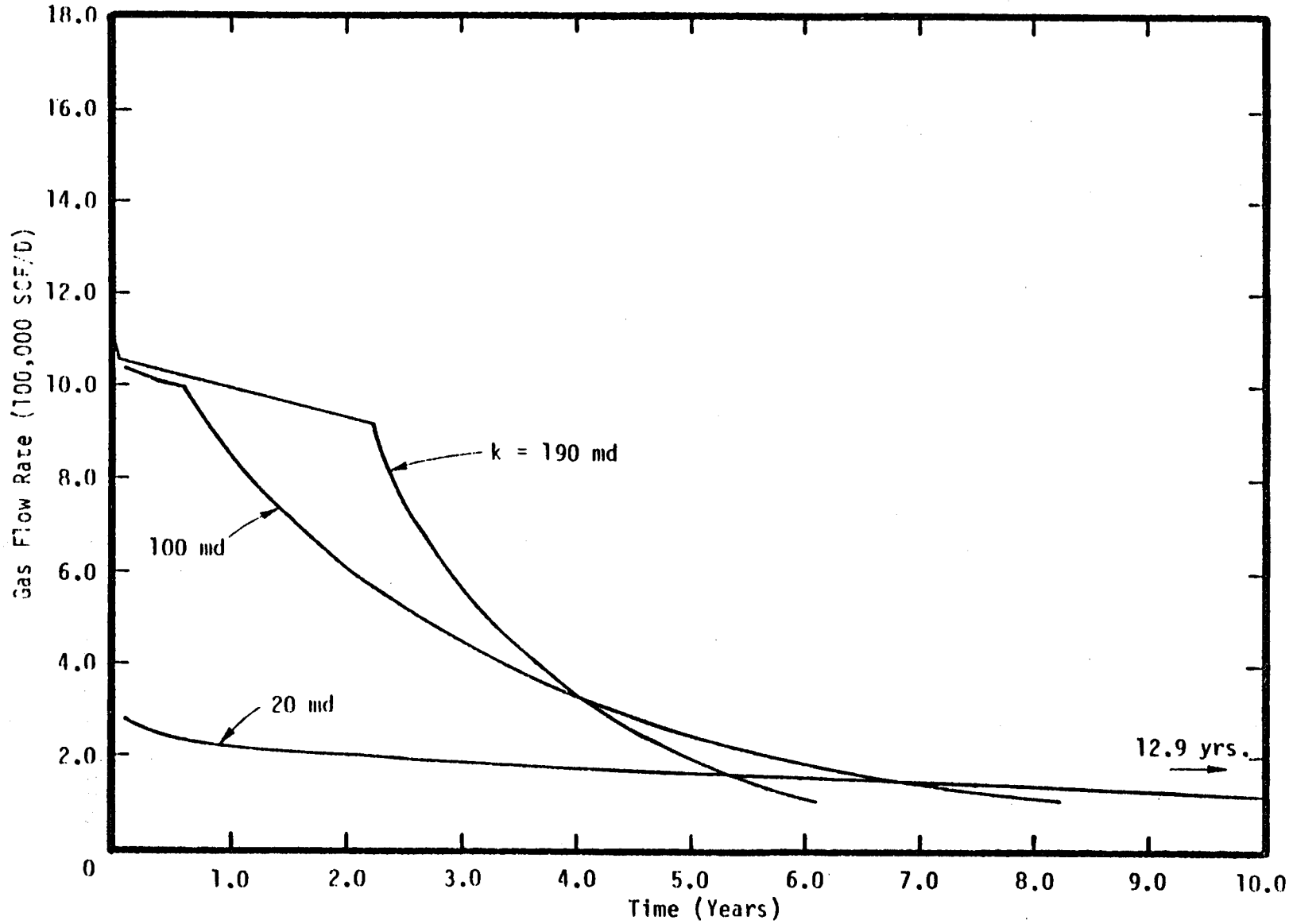

Figure 5. Effect of Formation Permeability on Gas-Production Rate

Table 3: Effect of Formation Permeability on Cumulative Brine and Methane Production

Formation Permeability (md)	Cumulative Brine Production (STB)	Cumulative Methane Production (SCF)	Average GWR SCF/STB
20	3.05×10^7 (1.65 percent)	7.37×10^8 (1.47 percent)	24.2
100	5.29×10^7 (2.87 percent)	1.235×10^9 (2.46 percent)	23.3
190	5.56×10^7 (3.02 percent)	1.306×10^9 (2.61 percent)	23.5

undersaturated or oversaturated with respect to methane. In order to assess the effect of reservoir gas content on the produced GWR, a series of three calculations (in addition to the base case) were run with the following values for methane mass fraction in the pore fluid:

1. C = 0.002716 (~ 24.5 SCF/STB), undersaturated
2. C = 0.007800, free gas volume fraction = 2.00 percent
3. C = 0.015276, free gas volume fraction = 5.01 percent.

The results of these calculations are shown in Figures 6 through 8 and in Table 4.

The sensitivity of bottom-hole pressure to gas content (Figure 6) is rather small. In all cases, the bottom-hole pressure declines to its minimum value in less than three years. The cumulative brine and methane production are essentially the same for both the undersaturated and the fully saturated cases. This is explained by the fact that, in the undersaturated case, the gas remains in solution until the brine becomes saturated at a lower pressure. For an initial free gas content of 2 percent, the total brine and gas produced are somewhat larger than the saturated case. This effect results from the pressure support provided by the free gas in the pores. In the latter case, the gas produced as a fraction of the gas in place is significantly less than that in the saturated case. Any gas evolved out of solution as a result of pressure decline stays in the reservoir pores, since the free gas saturation remains below the residual gas saturation. The calculated GWR for the highest initial gas saturation (~ 5.01 percent) is quite high. In this instance, since the initial free gas saturation is higher than the residual gas saturation, it is possible to mobilize the free gas (in excess of S_{gr}). The preceding results suggest that the produced GWR ratios are, in themselves, insufficient to differentiate between slightly undersaturated or slightly oversaturated geopressured reservoirs. Furthermore, the initial

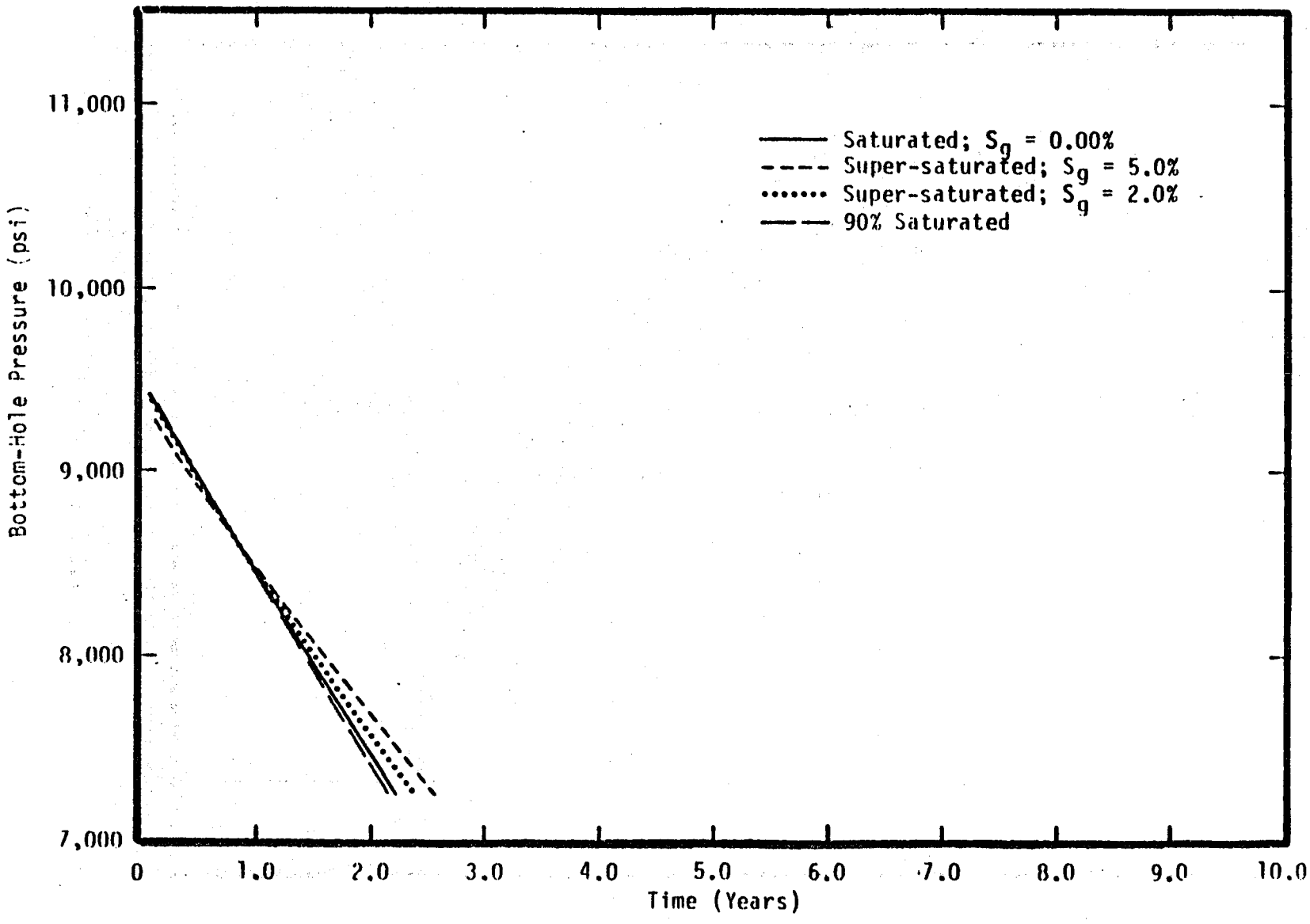

Figure 6. Sensitivity of Bottom-hole Pressure to Gas Content

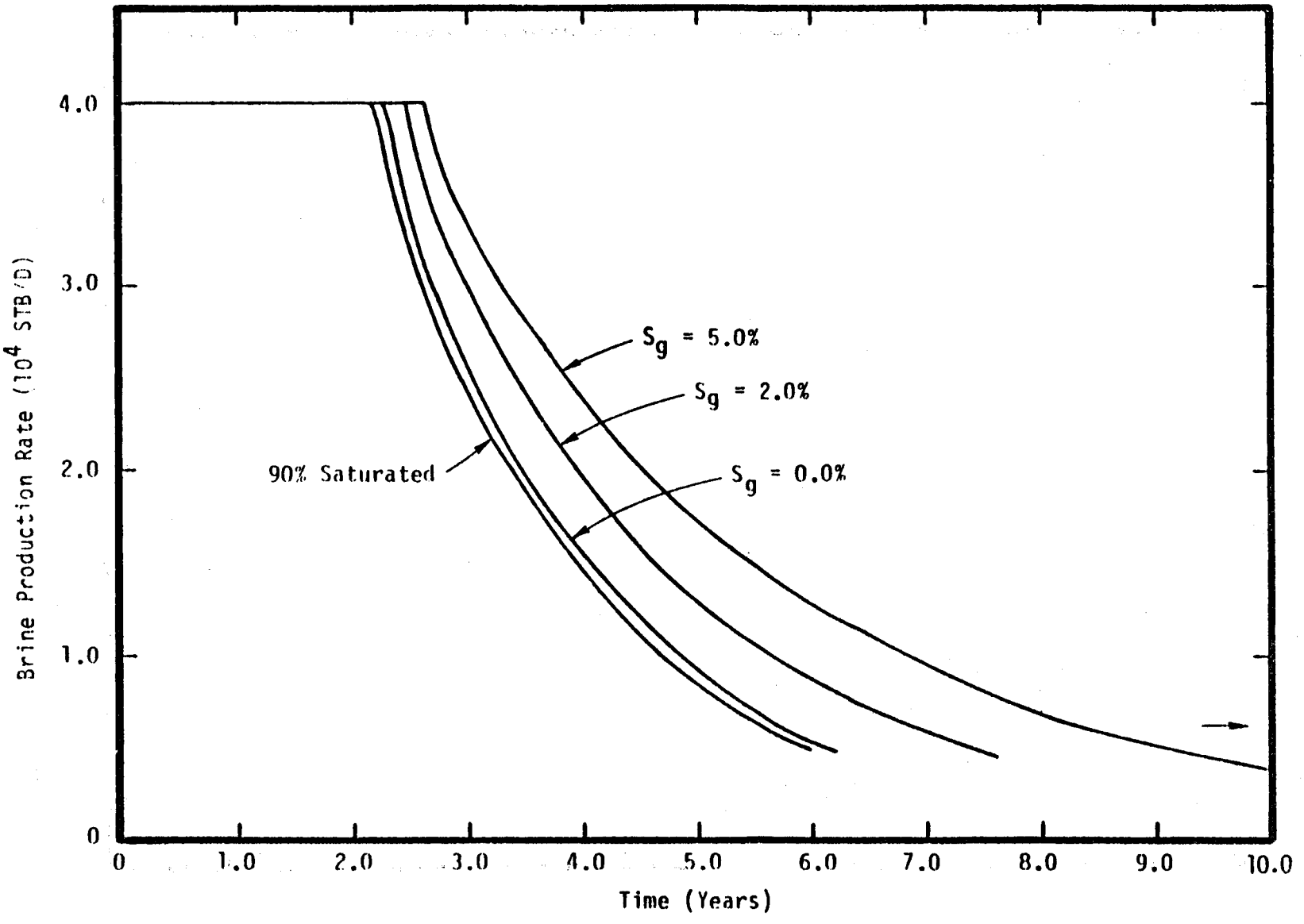

Figure 7. Sensitivity of Brine Production Rate to Gas Content

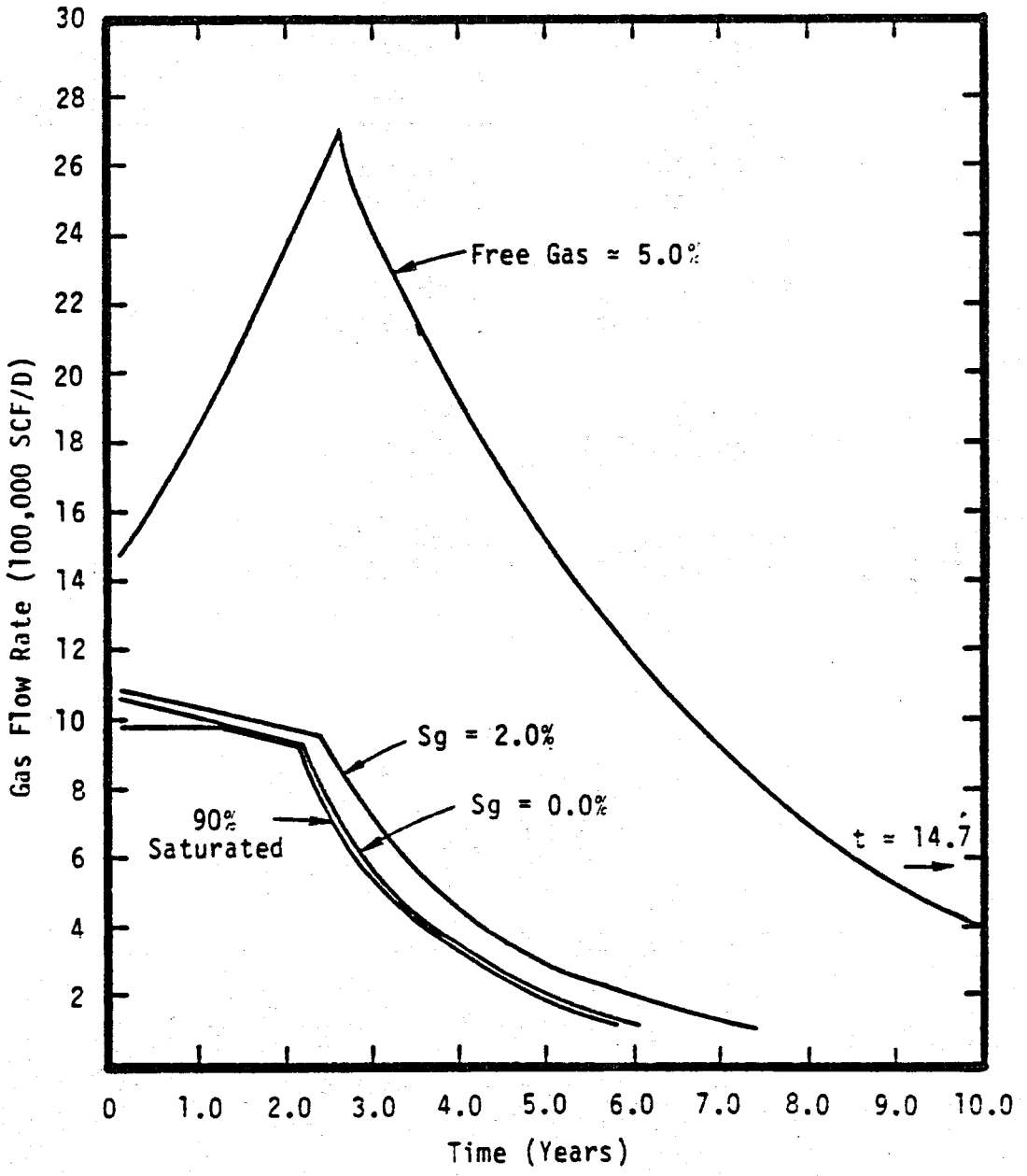

Figure 8. Sensitivity of Gas Production Rate to Gas Content

Table 4: Sensitivity of Cumulative Methane and Brine Production to Gas Content

Gas Content	Cumulative Brine Production (STB)	Cumulative Methane Production (SCF)	Average Produced GWR (SCF/STB)
Undersaturated (GWR ~ 24.5 SCF/STB)	5.41×10^7 (2.94 percent)	1.253×10^9 (2.78 percent)	23.2
Saturated (GWR ~ 27.2 SCF/STB)	5.56×10^7 (3.02 percent)	1.306×10^9 (2.61 percent)	23.5
Oversaturated (Free Gas ~ 2.00 percent)	6.42×10^7 (3.56 percent)	1.555×10^9 (1.22 percent)	24.2
Oversaturated (Free Gas ~ 5.01 percent)	7.98×10^7 (4.56 percent)	5.560×10^9 (2.28 percent)	69.7

free gas saturation must be either close to or more than S_{gr} for the produced gas water ratios to be above the saturation GWR. These conclusions are in agreement with those of the previously mentionedworks of Martin (1979) and Doscher, et al., (1982).

2.6 Salinity

The pore fluid salinity of geopressured aquifers varies over a wide range (See Section I). An increase in salinity leads to a decrease in the dissolved mass fraction of methane, and to an increase in fluid viscosity. To assess the sensitivity of reservoir production behavior to variations in fluid salinity, calculations were run for the following two (in addition to the base case) cases:

1. Total dissolved solids = 80,000 mg/L (s = 0.07594 gm/gm)
   Fluid viscosity = 0.238 cp
   Dissolved methane mass fraction, C = 0.003940 (= 34.4 SCF/STB)
   Initial Flow Rate = 40,000 STB/D (= 77.524 kg/s)
   Density of brine at standard conditions = 167.452 kg/STB

2. Total dissolved solids = 30,000 mg/L (s = 0.02943 gm/gm)
   Fluid viscosity = 0.211 cp
   Dissolved methane mass fraction, C = 0.005220 (= 44.2 SCF/STB)
   Initial Flow Rate = 40,000 STB/D (= 75.407 kg/s)
   Density of brine at standard conditions = 162.029 kg/STB

The results of these calculations are shown in Figures 9 through 11 and in Table 5.

A decrease in salinity results in the production of slightly larger fractions of brine (3.25 percent for 30,000 mg/L and 3.02 percent for 130,000 mg/L) and methane (2.81 percent for 30,000 mg/L and 2.61 percent for 130,000 mg/L) in place. This effect is principally due to an increase in the effective fluid compressibility with a decrease in the fluid salinity. The ratio of the produced GWR to the GWR in place is

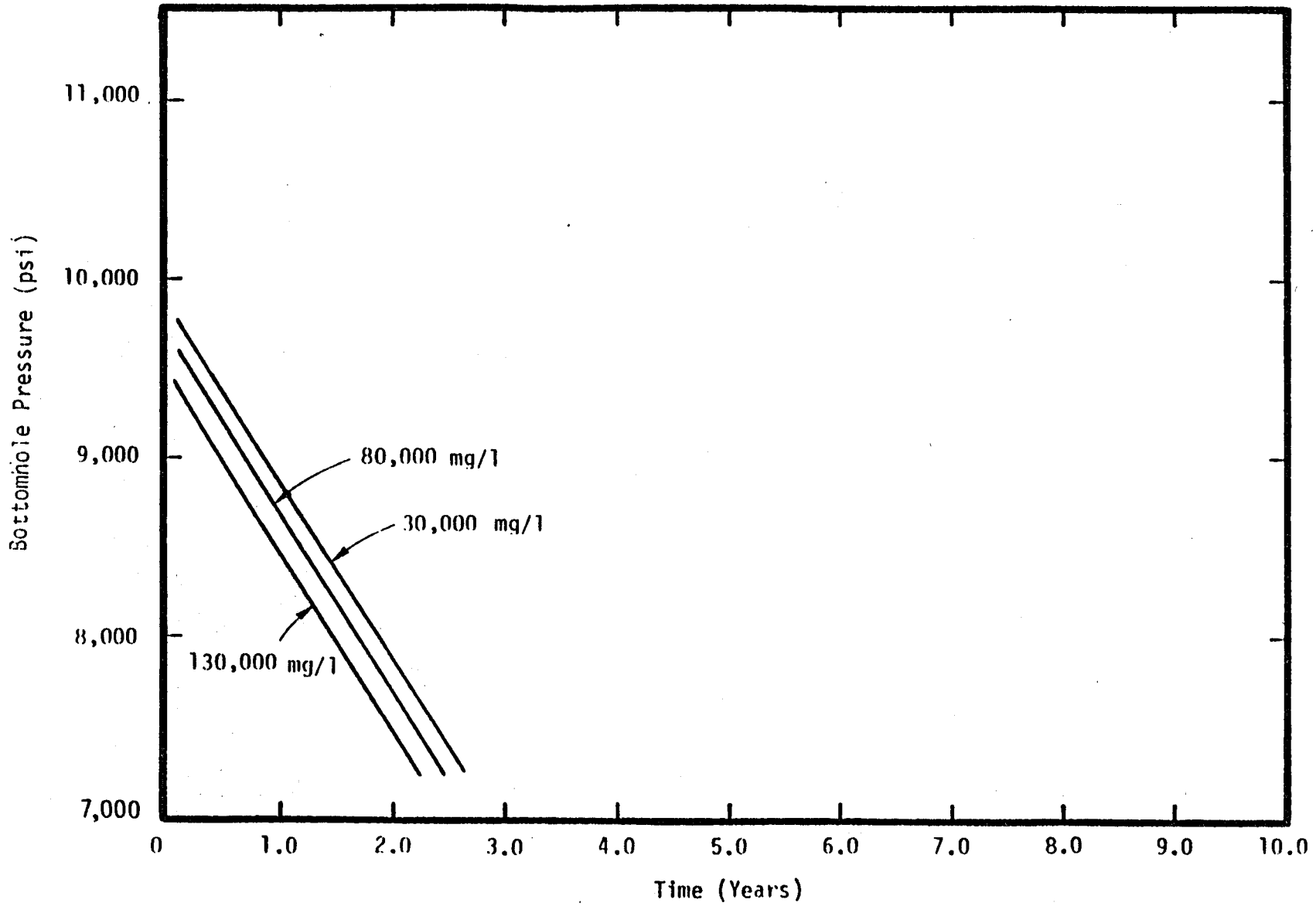

Figure 9. Effect of Pore Fluid Salinity on Bottom-hole Pressure

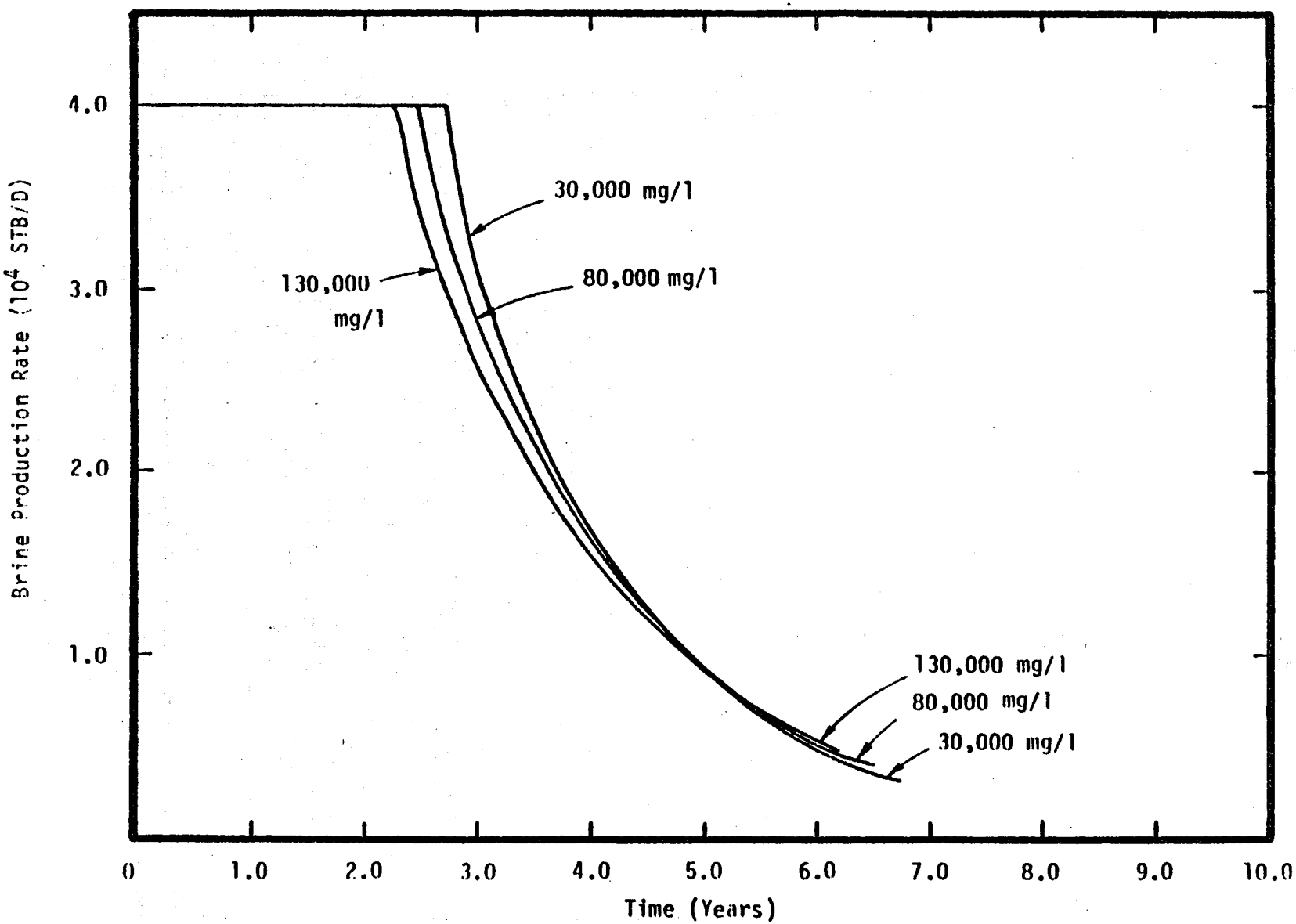

Figure 10. Effect of Pore Fluid Salinity on Brine Production Rate

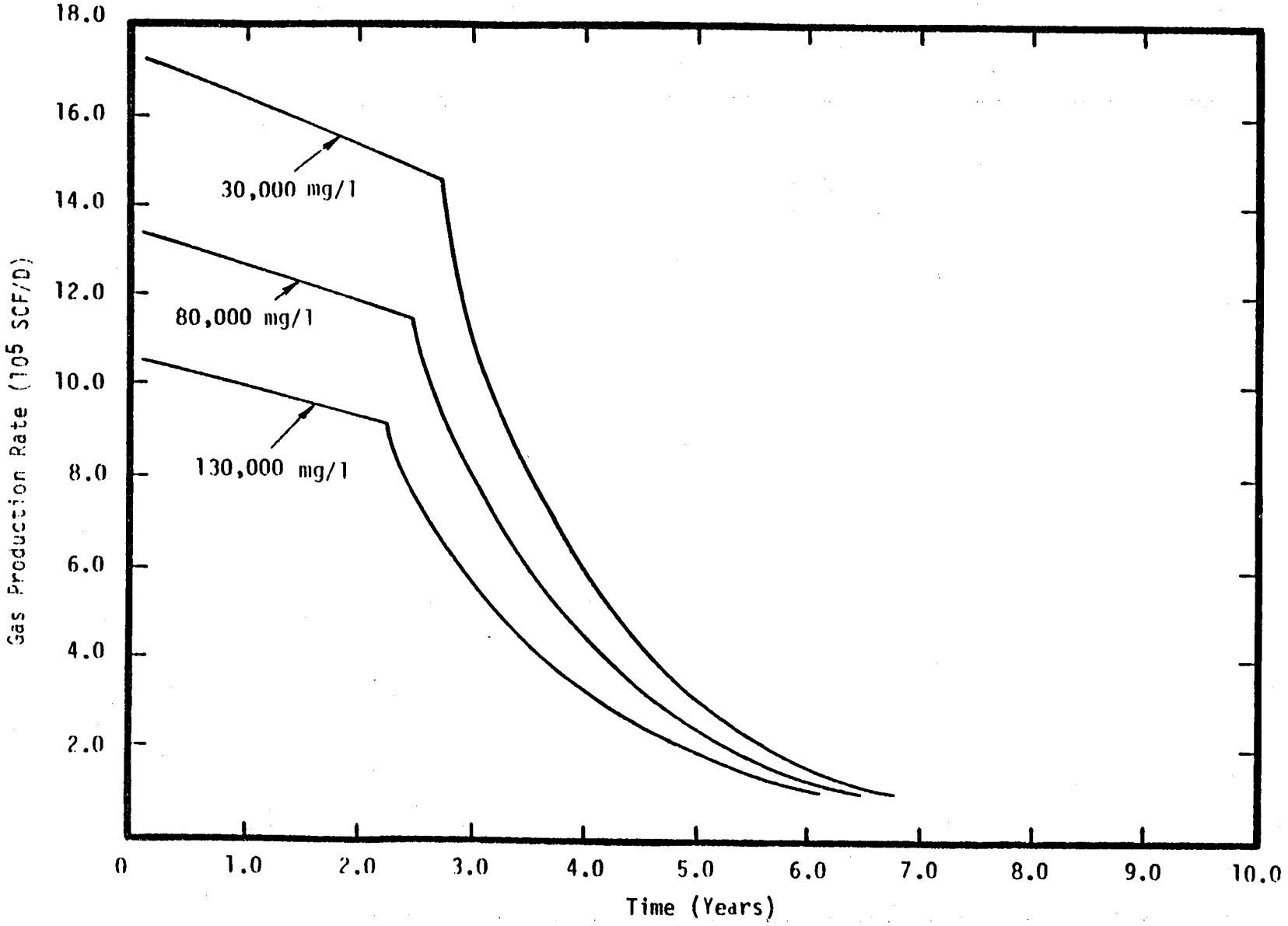

Figure 11. Effect of Pore Fluid Salinity on Gas Production Rate

Table 5. Effect of Pore Fluid Salinity on Cumulative Brine and Methane Production

Salinity (mg/L)	Cumulative Brine Production (STB)	Cumulative Methane Production (SCF)	Average GWR (SCF/STB)
30,000	5.93×10^7 (3.25 percent)	2.273×10^9 (2.81 percent)	38.3
80,000	5.75×10^7 (3.13 percent)	1.715×10^9 (2.71 percent)	29.8
130,000	5.56×10^7 (3.02 percent)	1.306×10^9 (2.61 percent)	23.5

essentially independent of fluid salinity, and is approximately 0.86. Finally Table 5 shows, as expected, that lower salinity results in a much larger cumulative methane production.

2.7 Pore Fluid Temperature

Results from the DOE well-test program show formation temperatures varying from 237°F to 327°F. To assess the sensitivity of reservoir production behavior to temperature, one calculation (besides the base case) was run with T = 250°F. A decrease in fluid temperature is accompanied by a decrease in dissolved methane content and an increase in fluid viscosity. For T = 250°F, we have:

Dissolved methane mass fraction, C = 0.002322 (≈ 20.9 SCF/STB)
Initial Flow Rate = 40,000 STB/D (≈ 80.186 kg/s)
Fluid Viscosity ≈ 0.330 cp.

The results of these calculations are given in Figures 12 through 14 and in Table 6.

It is clear from Table 6 that a decrease in formation temperature will result in a small decrease in cumulative brine production. The rather large decrease in cumulative methane production is of course a reflection of the smaller dissolved methane mass fraction.

2.8 Well Radius

To assess the effects of well radius, a single calculation was run with a well diameter of 5 1/2 in.; the results of this calculation are virtually indistinguishable from the base case. This is not surprising in view of the relatively large formation permeability (= 190 md) employed. The effects of well radius will become more pronounced with smaller formation permeabilities. The reduction of well diameter from 7 in. to 5-1/2 in. is equivalent to adding a positive skin of s = 0.24.

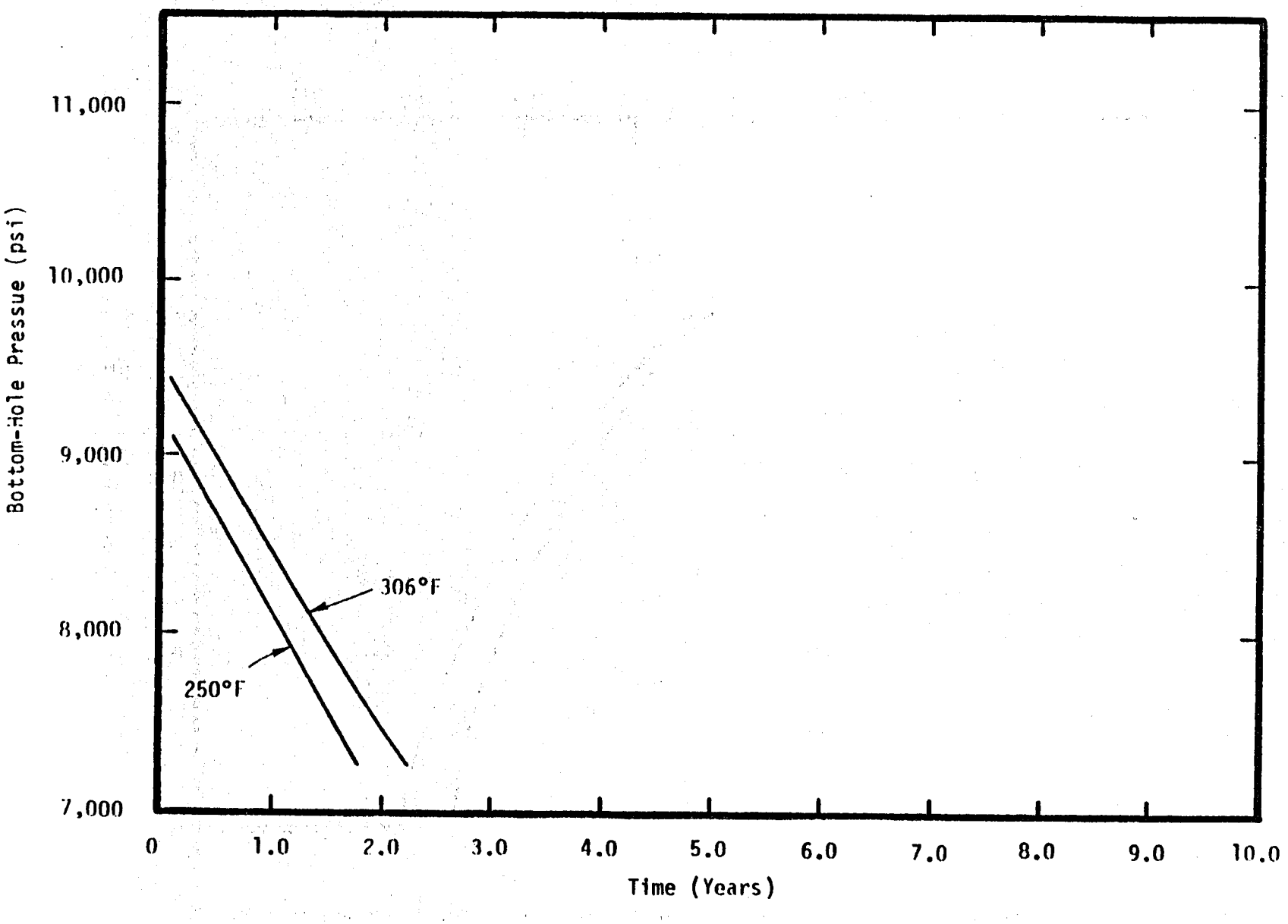

Figure 12. Sensitivity of Bottom-hole Pressure to Fluid Temperature

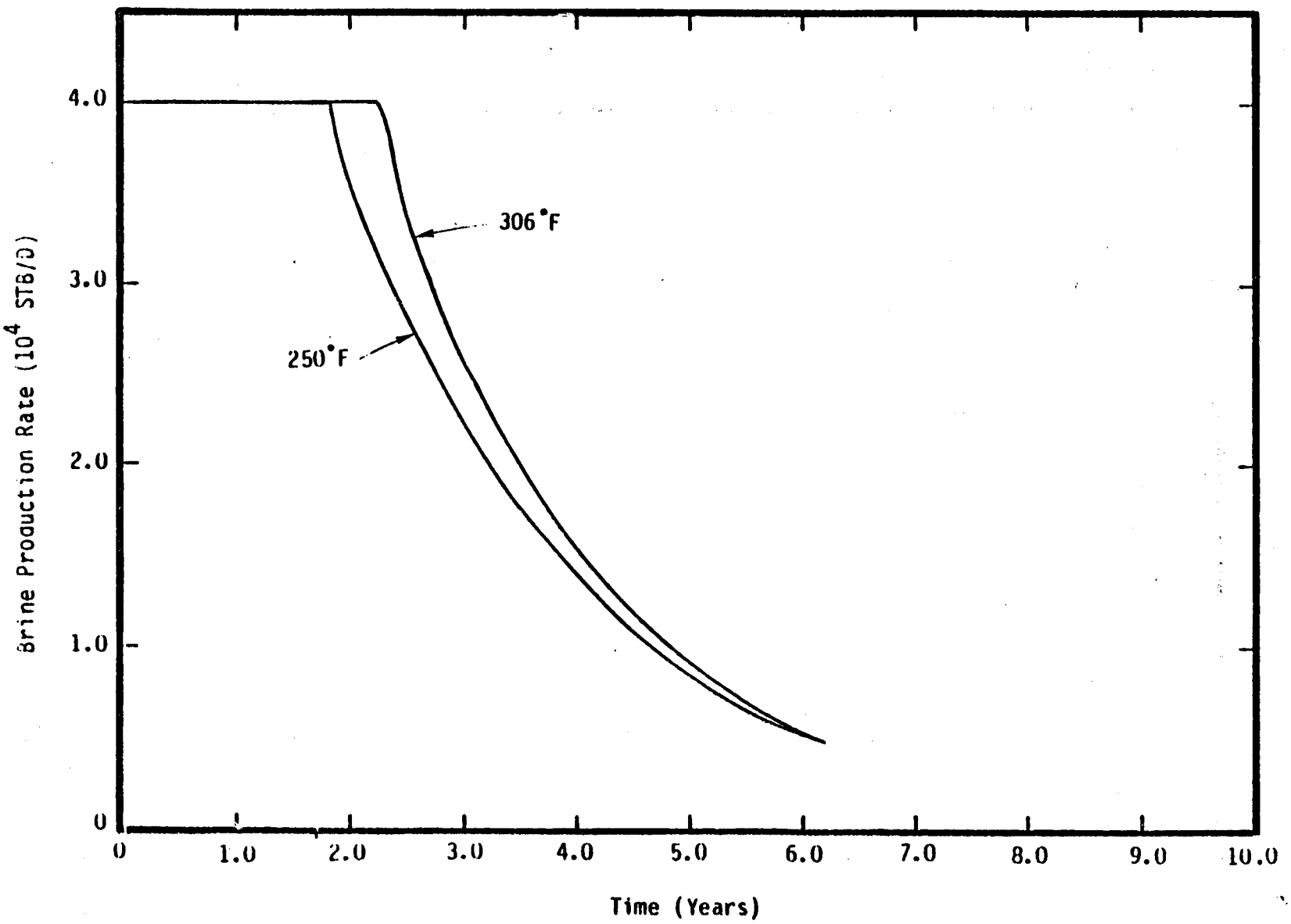

Figure 13. Sensitivity of Brine Production Rate to Fluid Temperature

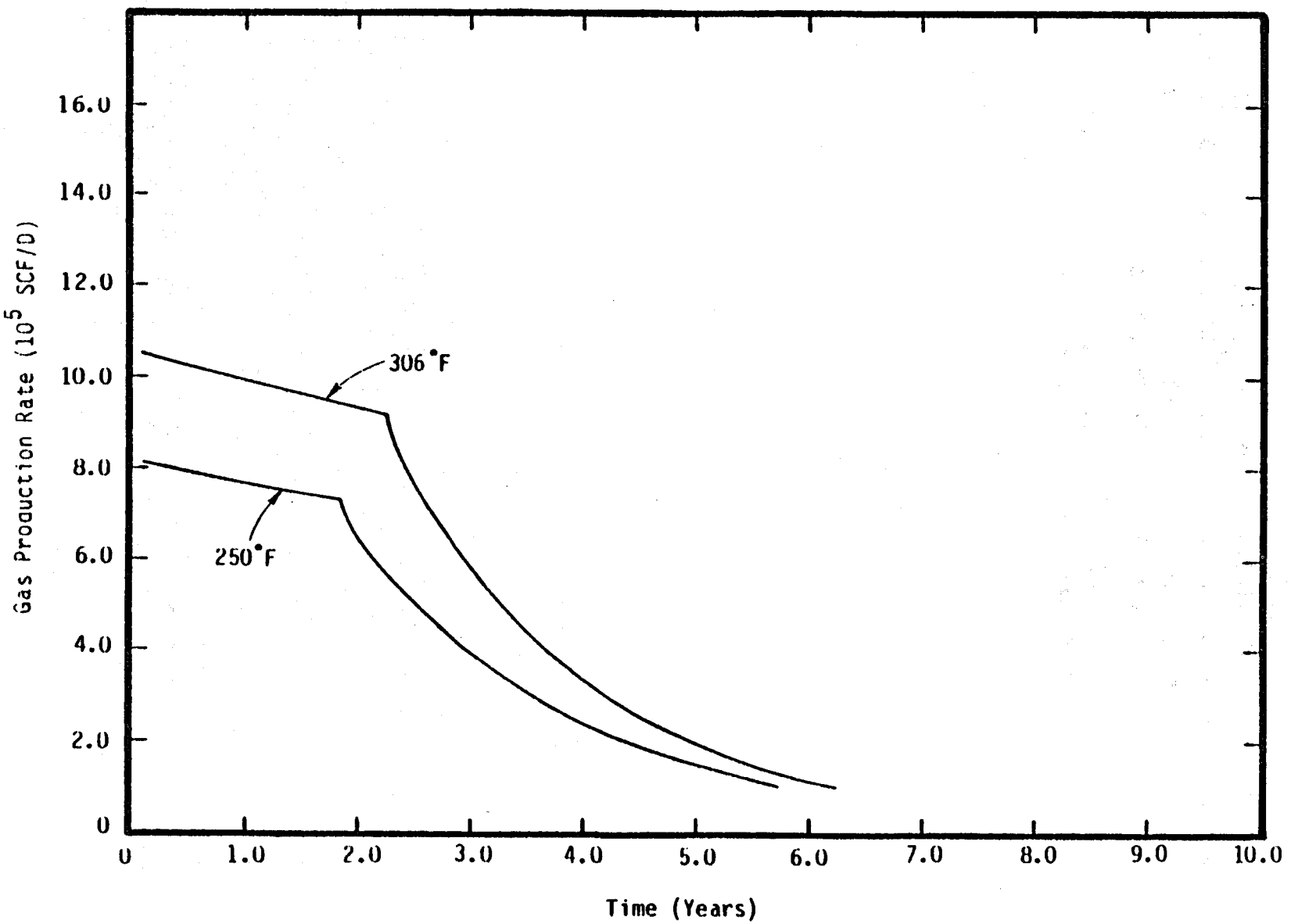

Figure 14. Sensitivity of Gas Production Rate to Fluid Temperature

Table 6. Sensitivity of Cumulative Brine and Methane Production to Variations in Fluid Temperature

Temperature (°F)	Cumulative Brine Production (STB)	Cumulative Methane Production (SCF)	Average GWR (SCF/STB)
250	5.13×10^7 (2.72 percent)	9.43×10^8 (2.39 percent)	18.4
306	5.56×10^7 (3.02 percent)	1.306×10^9 (2.61 percent)	23.5

$$s = \ln\left(\frac{7}{5.5}\right) \simeq 0.24$$

Pressure drop due to a skin of 0.24 and q = 40,000 STB/D is:

$$\Delta p_{skin} = \frac{141.3\ s\ q\ \mu\ B}{kh} \simeq 33 \text{ psi}$$

The above is clearly a negligible effect.

2.9 Well Location

In the base case, the well is located at 3000 ft from one boundary and at 21,000 ft from the remaining three boundaries. To investigate the effects of well location, a calculation was run with the well located at the geometric center of the reservoir (For this case an 8 x 11 numerical grid was employed with the well in the production block labeled as i = 8, j = 6. The grid in the i direction is identical with that shown in Figure 1. In the j direction, the following grid was used: $\Delta y_1 = \Delta y_2 = \Delta y_3 = \Delta y_4 = \Delta y_8 = \Delta y_9 = \Delta y_{10} = \Delta y_{11} = 2250$ ft, $\Delta y_5 = \Delta y_6 = \Delta y_7 = 2000$ ft.) The results for this case are compared with the base case in Figures 15 through 17 and in Table 7. It is apparent from these results that well location has a rather small effect on reservoir depletion behavior.

Pressure behavior in nonsymmetrical drainage areas (single-phase reservoirs) has been studied by Matthews, et al., (1954). During semi-steady reservoir response (depletion stage), the flowing pressure p_{wf} is given by

$$p_i - p_{wf} = \left[\frac{q\mu}{4\pi kh}\ \frac{4\pi kt}{\phi\mu C_T A} - \ln C_A + \ln\ \frac{A}{r_w^2} + 0.809 + 2s\right],$$

where

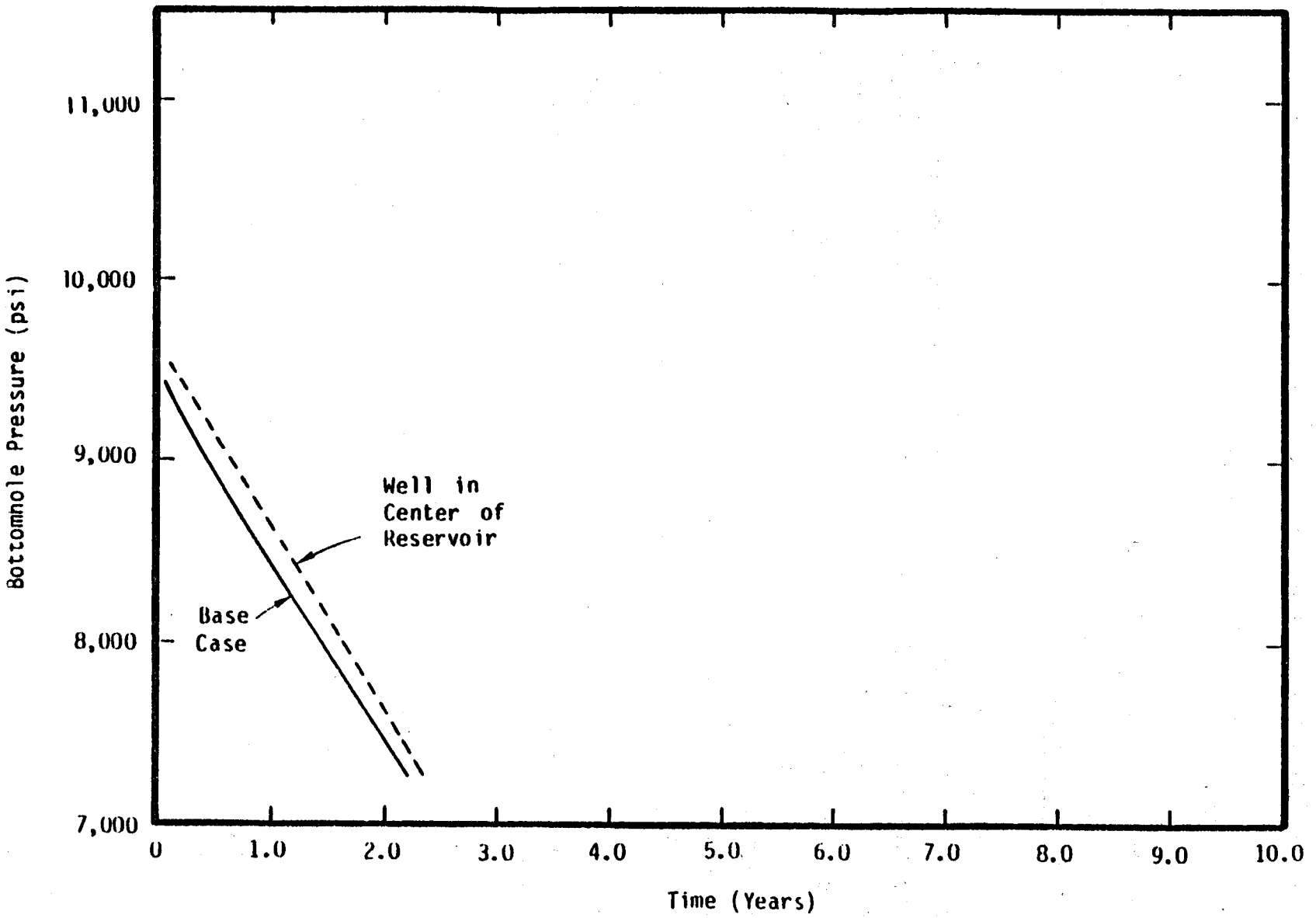

Figure 15. Effect of Well Locationn on Bottom-hole Pressure

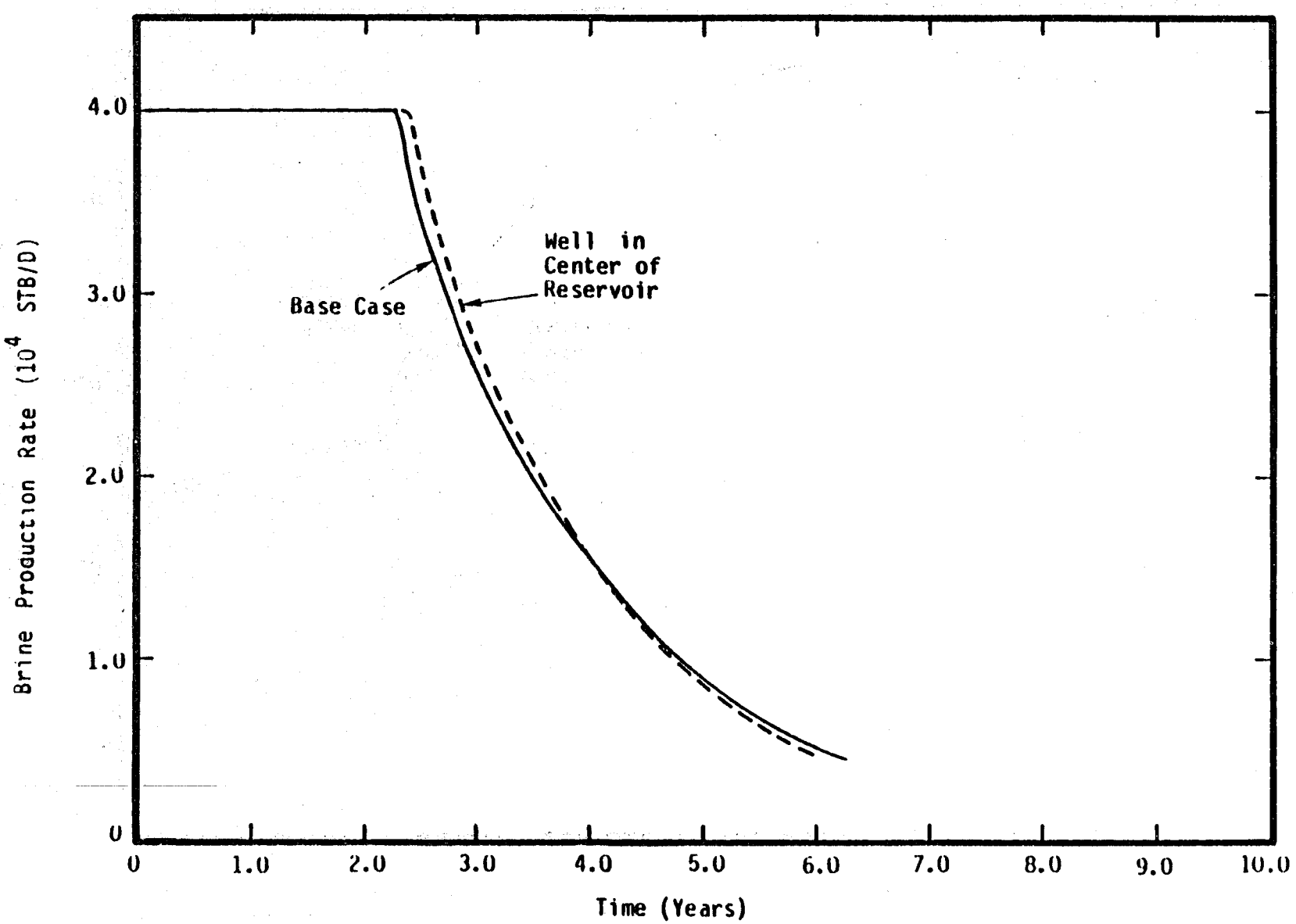

Figure 16. Effect of Well Location on Brine Production Rate

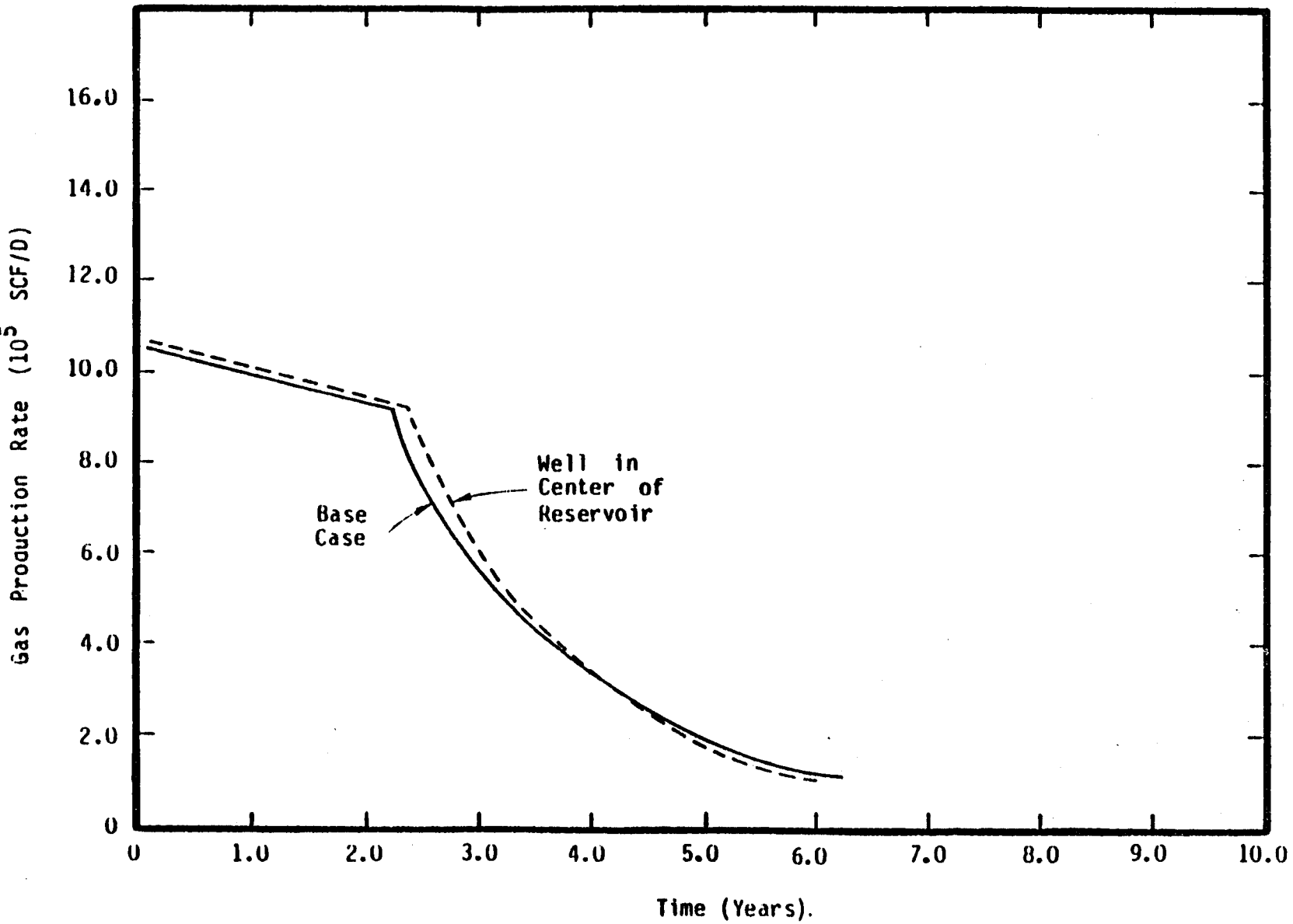

Figure 17. Effect of Well Location in Gas Production Rate

Table 7. Effect of Well Location on Cumulative Brine and Methane Production

Well Location	Cumulative Brine Production (STB)	Cumulative Methane Production (SCF)	Average GWR (SCF/STB)
Base Case	5.56×10^7 (3.02 percent)	1.306×10^9 (≈ 2.61 percent)	23.5
Geometric Center of Reservoir	5.59×10^7 (3.03 percent)	1.326×10^9 (2.65 percent)	23.7

q = flow rate in m^3/s
k = formation permeability in m^2
h = formation thickness in m^2
t = flowing time in sec
ϕ = porosity
μ = fluid viscosity in Pa-s
C_T = total formation compressibility in Pa^{-1}
A = drainage area in m^2
C_A = shape factor
r_w = wellbore radius in m
s = skin factor

With the parameter values used in the present calculations (k = 190 md $\simeq$ 190 x 10^{-15} m^2, t = 5 years $\simeq$ 1.577 x 10^8 s, ϕ = 0.18, μ = 0.267 cp = 0.267 x 10^{-3} Pa-s, C_T = 7.56 x 10^{-6} psi^{-1} $\simeq$ 1.0965 x 10^{-9} Pa^{-1}, A = 1.008 x 10^9 ft^2 $\simeq$ 9.365 x 10^7 m^2, r_w = 3.5 in. = 0.0889 m, s = 0), we have:

$$p_i - p_{wf} \simeq \frac{q\mu}{4\pi kh} [100.3 - \ln C_A]$$

Since $\ln C_A$ is of the order of unity it is obvious that well location, vis a vis reservoir boundaries, is not critical in this case. The effects of well location will become more pronounced with a decrease in formation permeability. Thus, for example, with k = 10 md, the flowing pressure p_{wf} is given by

$$p_i - p_{wf} \simeq \frac{q\mu}{4\pi kh} [28.0 - \ln C_A]$$

2.10 Maximum (Initial) Flow Rate

Efficient generation of electric power from geopressured brine requires that the brine be supplied at a nearly constant rate to the power plant. The latter requirement may be in conflict with the most

economic (usually over as short period of time as possible) recovery of gas. To assess the sensitivity of reservoir production behavior to variations in the maximum desired (i.e., initial) flow rate, two calculations were carried out with initial flow rate set at 30,000 bbl/D and 20,000 bbl/D. The results of these calculations are compared with the base case in Figures 18 through 20 and in Table 8.

The cumulative volumes of brine and methane produced in all three cases are practically identical; for q = 20,000 bbl/D, it will take, however, considerably longer (~ 9 years versus ~ 6 years) to produce the reservoir than for q = 40,000 bbl/D. A rate of 40,000 bbl/D can only be maintained for slightly over two years whereas a rate of 20,000 bbl/D can be sustained for nearly 6.5 years. It would therefore appear more efficient (as far as electric power generation is concerned) to operate the reservoir at the lower rate. The possibility of producing a greater amount of electric power will, however, need to be weighed against the increased operating costs incurred when production operations are extended for a longer period of time.

2.11 Shale Recharge

Sandstone reservoirs having the greatest potential for development are most likely to occur within the alternating sandstone and shale facies. Although the shales which contain the bulk of the fluid resource have permeabilities too low to allow their direct development for fluid production, it is possible that the shales may yield significant quantitites of brine to the permeable sandstones when subjected to production stress (i.e., a pressure gradient across the shale/sandstone interface). Further, most Gulf Coast shales are impure in that they contain varying amounts of silt size particles. The shales could, therefore, act as sources of recharge for the sandstones, permitting greater fluid recovery than that obtainable by pressure depletion of the sandstone reservoirs alone.

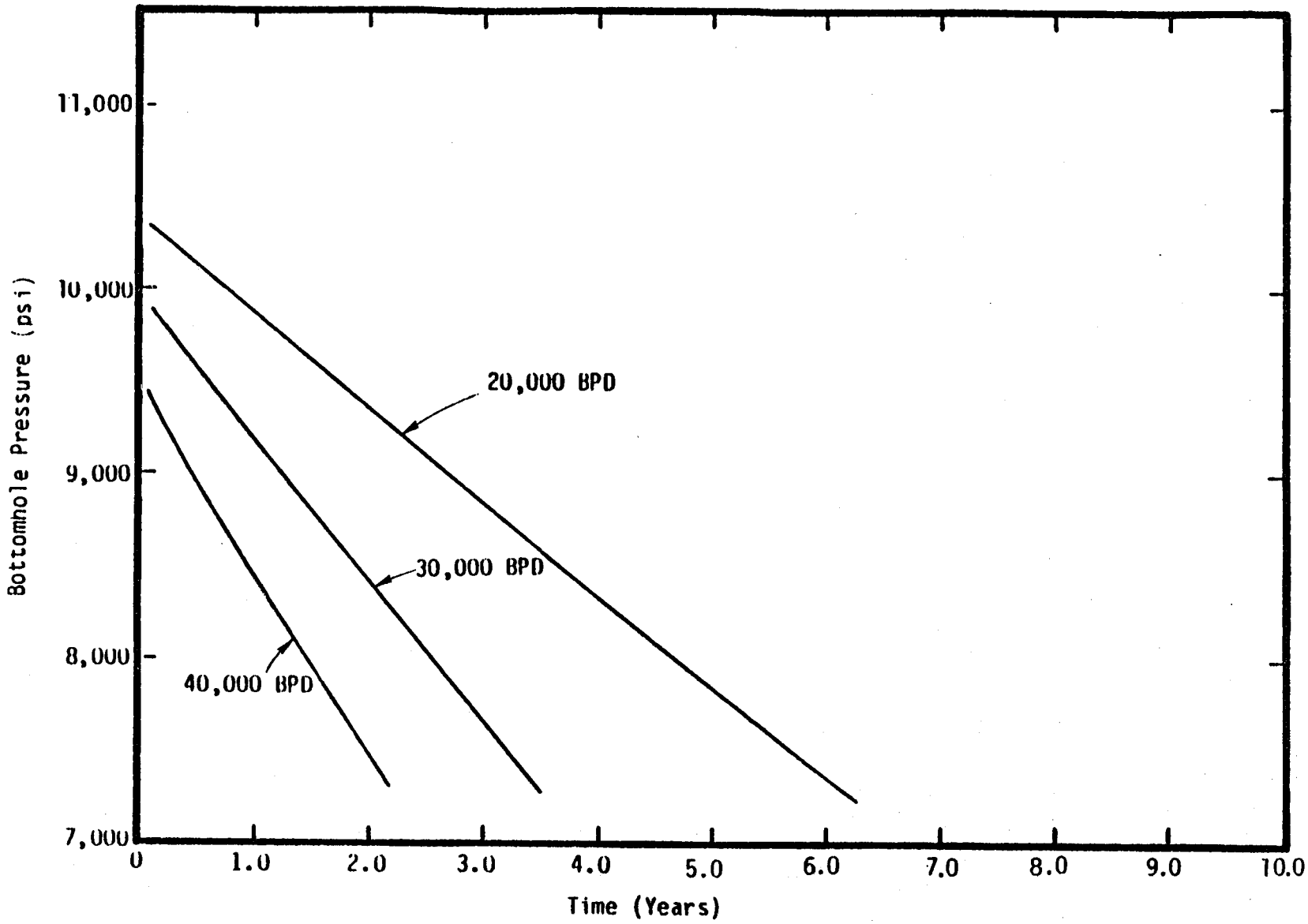

Figure 18. Sensitivity of Bottom-hole Pressure to Maximum (Initial) Flow Rate

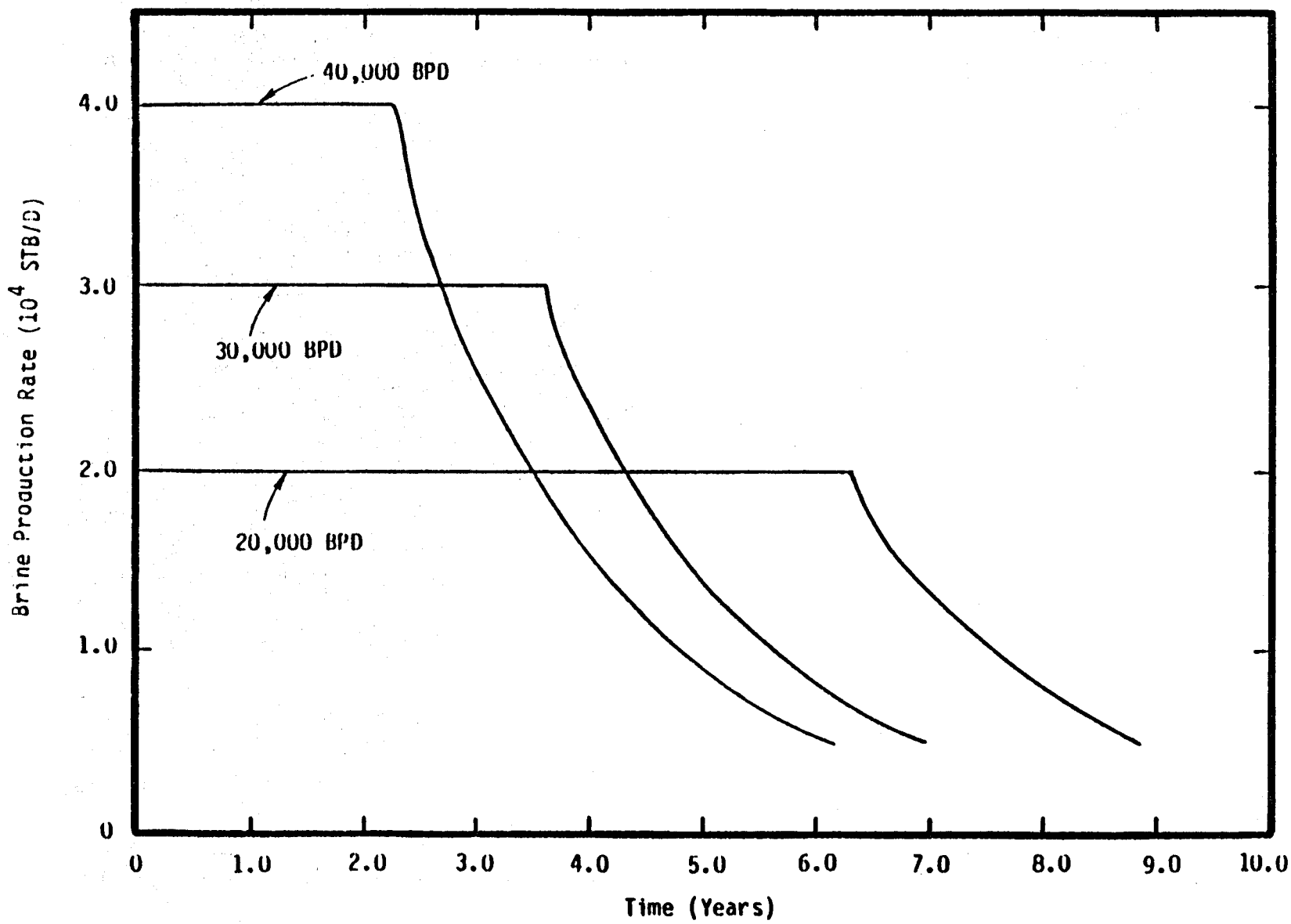

Figure 19. Sensitivity of Brine Production Rate to Maximum (Initial) Flow Rate

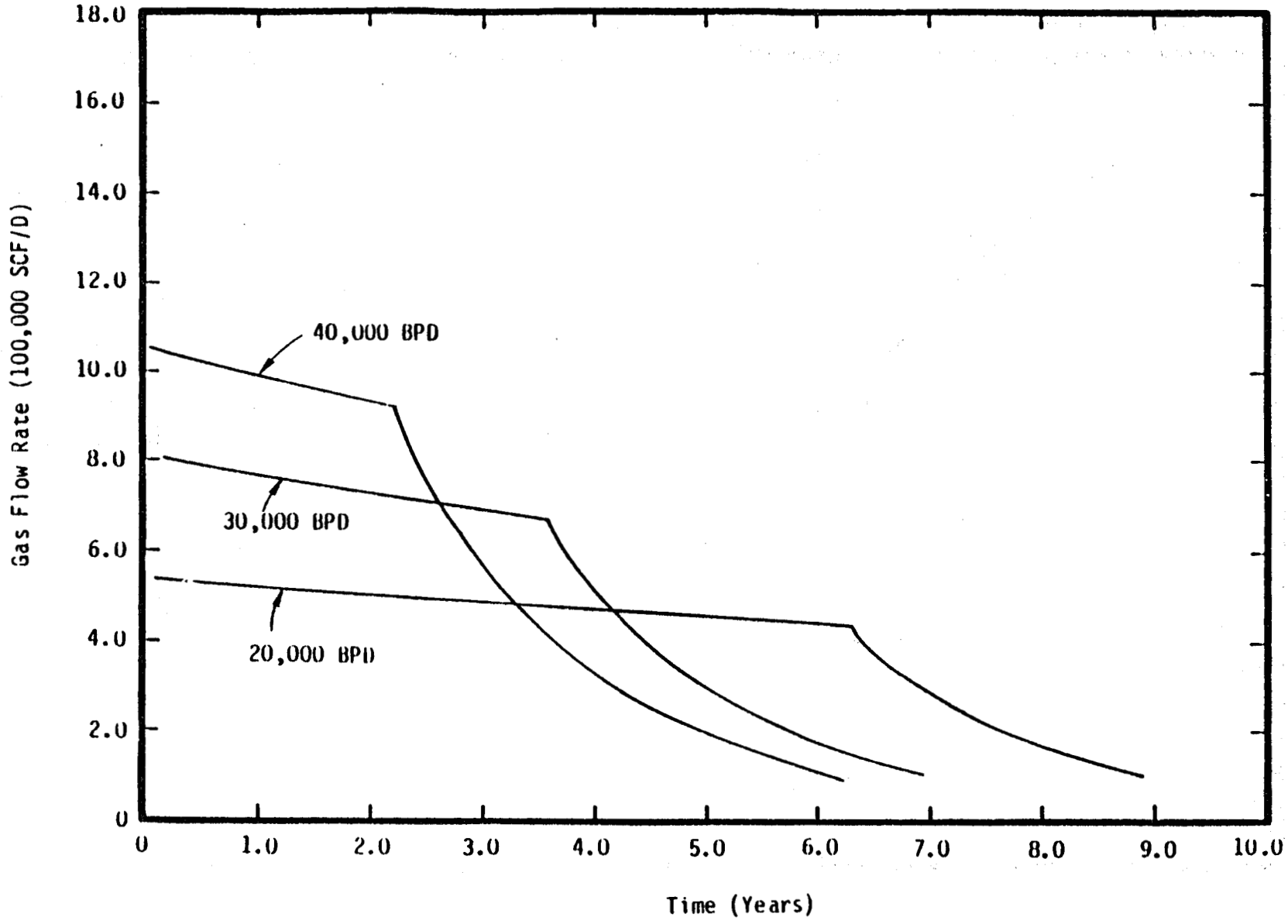

Figure 20. Sensitivity of Gas Production Rate to Maximum (Initial) Flow Rate

Table 8. Sensitivity of Cumulative Brine and Methane Production to Variations in the Maximum Flow Rate

Maximum Flow Rate (BPD)	Cumulative Brine Production (STB)	Cumulative Methane Production (SCF)	Average GWR (SCF/STB)
20,000	5.55×10^7 (3.02 percent)	1.321×10^9 (2.64 percent)	23.8
30,000	5.55×10^7 (3.02 percent)	1.314×10^9 (2.62 percent)	23.7
40,000	5.56×10^7 (3.02 percent)	1.306×10^9 (2.61 percent)	23.5

The concept of shale recharge was apparently first discussed by Wallace (1968). According to Wallace, shale water influx is governed by (1) the permeability (especially vertical) and compressibility of the shales, (2) the pressure differential across the shale/ sandstone interface, and (3) the contact area of the sand/shale interface.

For geopressured-geothermal reservoirs, shale water influx has previously been theoretically investigated by Garg, et al., (1978), Pritchett, et al., (1979) and Garg, et al., (1980). Garg, et al., (1980) concluded that significant shale recharge will take place only if the vertical shale permeability is at least of the order of $0.01\mu d (\sim 10^{-5} md)$. Also for vertical shale permeabilities of the order of $0.01\mu d$, shale-water influx effects would become apparent only for production times longer than two to three years. Since, up to the present time, no geopressured-geothermal well has been flow tested for more than a few months, there has been little opportunity to observe shale-water recharge in geopressured aquifers. (Although there exists some evidence of fluid recharge in the Dow-DOE Sweezy No. 1 well, at present it is uncertain whether the apparent fluid recharge comes from a leaky boundary or from the adjoining shales.) Another difficulty in assessing the importance of shale-water influx in geopressured aquifers is the current paucity of data on the relevant shale properties (permeability, compressibility and thickness, etc.).

To characterize the effects of shale-water recharge, a 60 ft thick sand sandwiched between two 60 ft thick shale layers was considered. In the interest of minimizing computational costs, the sand/shale reservoir system was assumed to be a right circular cylinder with radius $R \sim 1.7912 \times 10^4$ ft (corresponding to a block area of 1.008×10^9 ft^2 used in the calculations discussed in the preceding sections) and with the production well located at the geometric center of the reservoir. For this case, a 21 x 6 numerical grid was employed. In the radial or i direction a uniform grid spacing of 792.48 ft (260 m) was used. Because of symmetry in the

vertical (or z direction), it is sufficient to consider the half of the sand-shale system which lies above the plane of symmetry. In the z-direction, the sand-shale system was simulated by using the following grid: $\Delta z_1 = 30$ ft, $\Delta z_2 = \Delta z_3 = 5$ ft, $\Delta z_4 = 10$ ft, $\Delta z_5 = \Delta z_6 = 20$ ft. A single grid block (Δz_1) is employed for the sand half-layer. The shale layer is, however, approximated by five grid blocks. Fine spatial resolution (in the shale layer) is required near the sand/shale interface to accurately resolve the large pressure-gradient at this interface. The sand/shale properties, with a few exceptions (vertical sand/shale permeabilities, shale compressibility, and horizontal shale permeability), are taken to be the same as those for the base case sands. The sand and shale permeabilities, and shale compressibility, for the five cases considered are given in Table 9. Note that Case 1 is the same (apart from the reservoir geometry) as the base case. Apart from the vertical shale permeability and shale compressibility, the other properties are assumed to be the same in all the five cases.

Hantush (1964) presents an analytical solution for constant rate fluid production from a layered (semi-pervious aquitard overlying an aquifer) reservoir system of infinite lateral extent. The analysis is based on the assumption that the flow in the aquitard (or shale layer) is vertical and the flow in the aquifer (or sand layer) may be treated as horizontal and radial. In addition, the pore fluid is taken to be single phase and the formation properties are regarded as simple constants (in other words, a change in porosity and hence permeability with a drop in pore pressure is excluded). The Appendix to this report treats the case of fluid production from a layered reservoir system of finite lateral extent. The various simplifying assumptions (e.g. single phase flow, constant formation properties) necessary to obtain this semi-analytical solution imply that this solution cannot be used to quantitatively evaluate shale-water recharge. Nevertheless, the solution is useful for determining the accuracy of numerical solutions obtained through the use of the

Table 9. Sand/Shale Properties

Case	Horizontal Shale Permeability (md)	Vertical Shale Permeability (md)	Horizontal Sand Permeability (md)	Vertical Sand Permeability (md)	Uniaxial Shale Compressibility (psi^{-1})
1	0	0	190	(Not Applicable)	
2	10^{-4}	10^{-5}	190	19	10^{-5}
3	10^{-4}	10^{-4}	190	19	10^{-5}
4	10^{-4}	10^{-5}	190	19	10^{-6}
5	10^{-4}	10^{-5}	190	19	10^{-4}

reservoir simulator MUSHRM. Figure 21 compares the bottom-hole pressures (Cases 2 and 3, Table 9) given by the two methods. For the MUSHRM calculations (Figure 21), the reservoir brine was assumed to be devoid of methane and the permeabilities were taken to be independent of porosity (and hence pore pressure). The rather excellent agreement between the numerical and semi-analytical solutions indicates that the vertical spatial resolution used near the sand/shale interface is sufficient to obtain accurate numerical solutions.

The results of the calculations for the five cases of Table 9 are shown in Figures 22 through 24 and summarized in Table 10. (For these calculations, unlike those presented in Figure 21, the reservoir brine is assumed to be saturated with methane and the permeability is allowed to vary with porosity. The brine in the sand and shale layers is assumed to have the same initial properties.) Comparison of Cases 1, 2 and 3 shows that for vertical permeabilities exceeding 10^{-5} md, significantly more gas and brine will be recovered than for the no shale recharge case. As a matter of fact, for shale vertical permeability equal to both 10^{-5} and 10^{-4} md, the well was producing in excess of the minimum allowed gas production rate (100,000 SCF/D) at t = 30 years when the calculations were terminated. For shale vertical permeability $k_{v,sh} = 10^{-5}$ md, the brine and gas production at 30 years are 9030 STB/D and 191,700 SCF/D respectively. The brine production rate in the high permeability case (Case 3) stays at 40,000 STB/D for approximately 16.5 years. It then slowly declines to 25,070 STB/D at t = 30 years. The gas production rate at the latter time is 556,200 SCF/D. These calculations also suggest that for vertical shale permeability of the order of 10^{-5} md the effects of shale recharge on bottom-hole pressure will not become apparent for production times less than several months (see Figure 22). The exact value of the critical production time decreases with an increase in the vertical shale permeability.

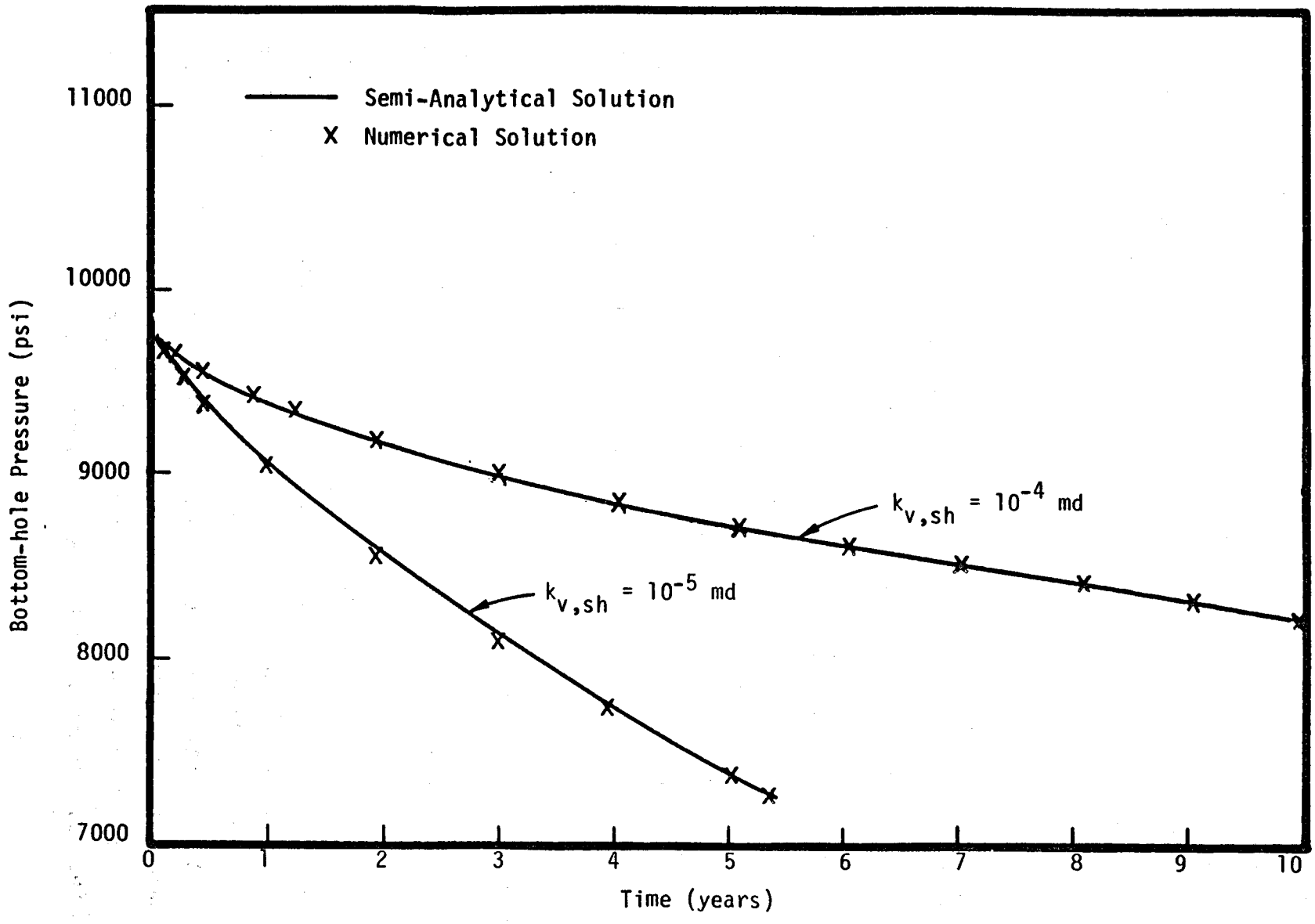

Figure 21. Comparison of Numerical Solution with Semi-Analytical Solution

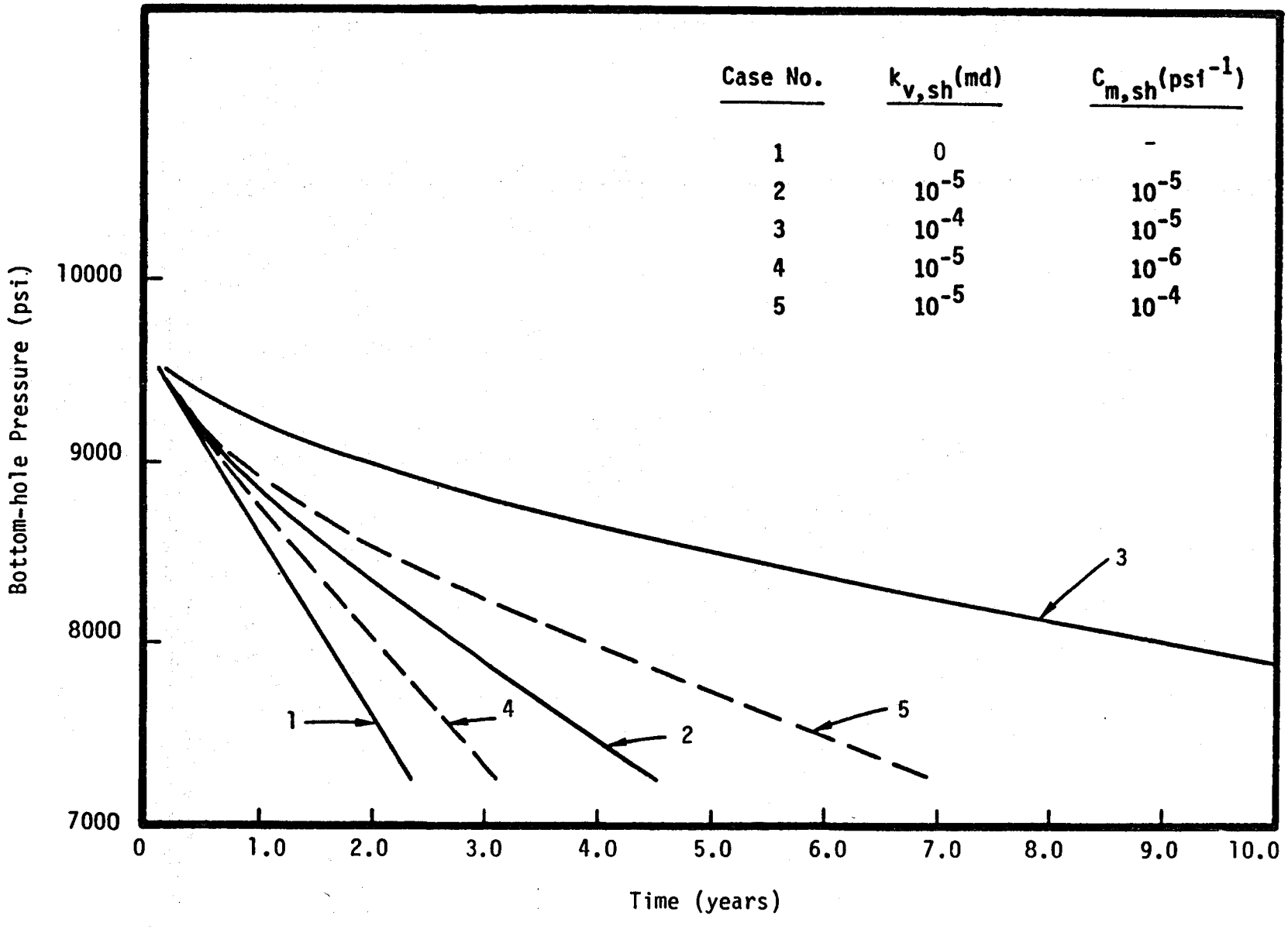

Figure 22. Sensitivity of Bottom-hole Pressure to Vertical Shale Permeability and Shale Compressibility

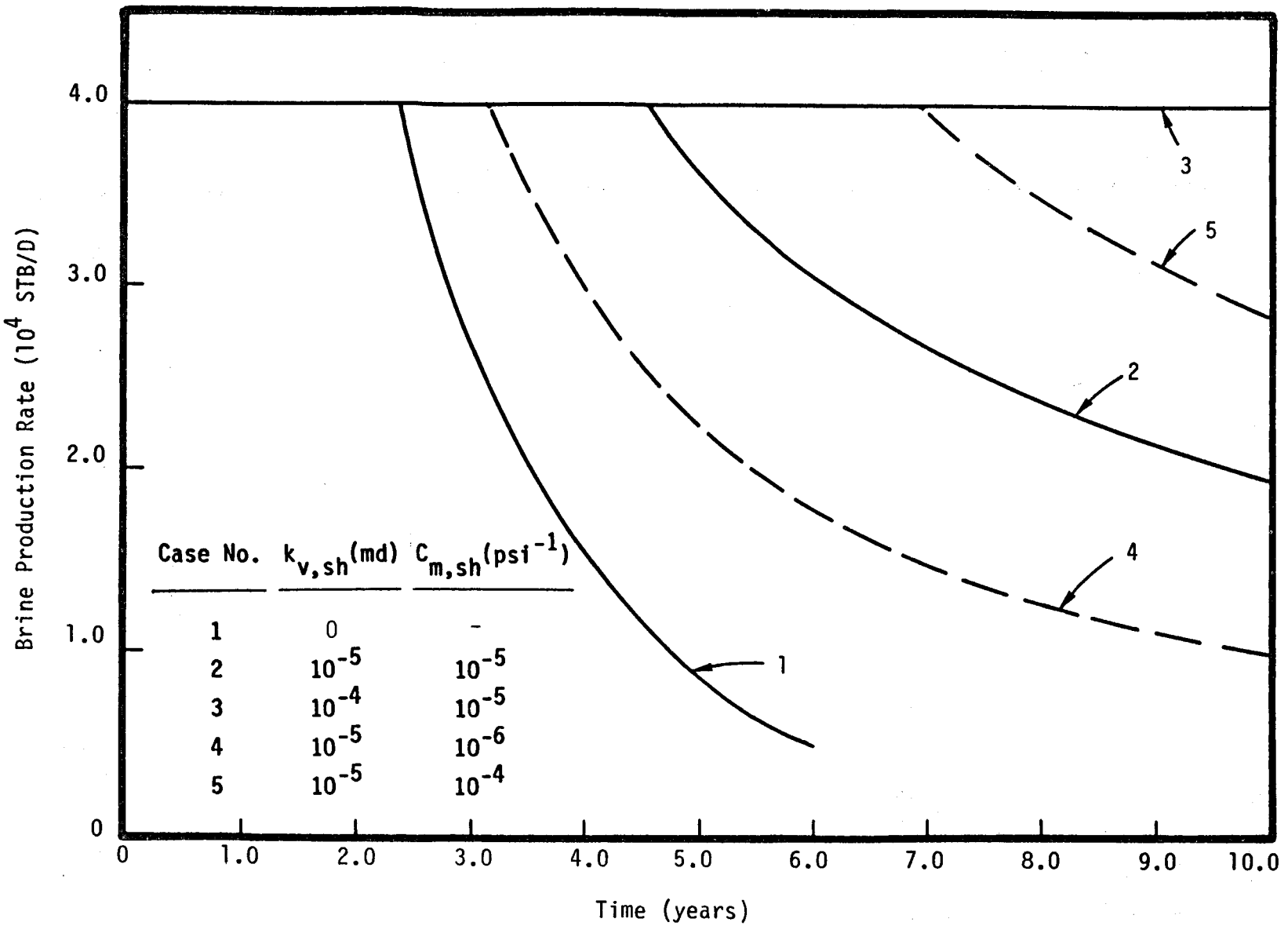

Figure 23. Sensitivity of Brine Production Rate to Vertical Shale Permeability and Shale Compressibility

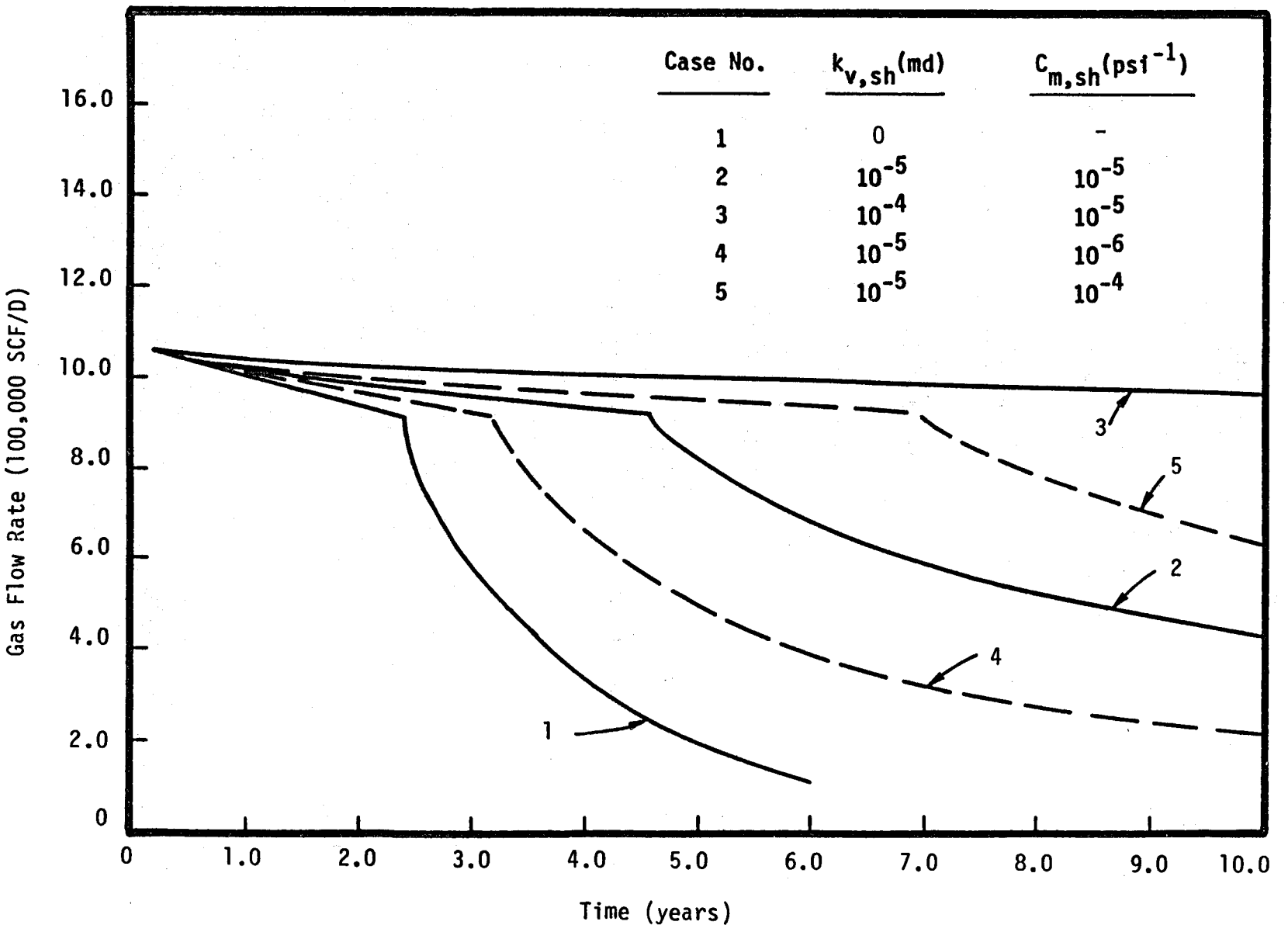

Figure 24. Sensitivity of Gas Production Rate to Vertical Shale Permeability and Shale Compressibility

Table 10. Sensitivity of Cumulative Brine and Methane Production to Vertical Shale Permeability and Uniaxial Shale Compressibility

Vertical Shale Permeability (md)	Uniaxial Shale Compressibility (psi^{-1})	Cumulative Brine Production (STB)	Cumulative Methane Production (SCF)	Average GWR (SCF/STB)
0	Not Applicable	5.564×10^{7} ● (3.02 percent)	1.316×10^{9} ● (2.63 percent)	23.7
10^{-5}	10^{-5}	2.104×10^{8} * (11.42 percent)	4.762×10^{9} * (9.50 percent)	22.6
10^{-4}	10^{-5}	3.950×10^{8} * (21.44 percent)	9.360×10^{9} * (18.68 percent)	23.7
10^{-5}	10^{-6}	1.243×10^{8} ** (6.75 percent)	2.824×10^{9} ** (5.64 percent)	22.7
10^{-5}	10^{-4}	2.475×10^{8} * (13.43 percent)	5.680×10^{9} * (11.34 percent)	22.9

Production at: ● = 6.0 years, * = 30.0 years, ** = 23.5 years.

Cases 4 and 5 were designed to assess the effects of shale compressibility on shale-water influx. Comparison of Cases 2, 4 and 5 shows that an increase in shale compressibility leads to an increase in both brine and gas recovery. This increase in brine and gas production is, however, not as great as that predicted by the semi-analytical solution (see Appendix). The semi-analytical solution implies that a ten-fold increase in vertical shale permeability has the same effect as a ten-fold increase in shale compressibility. If this were true in the present case, the results for Cases 3 and 4 would be essentially identical; this is not so. The reason for this divergence is fairly straightforward. The numerical model used in this work incorporates a nonlinear relationship between permeability and porosity (and implicitly pore pressure). Shale-water influx is accompanied by a drop in pore pressure in the shale layer; this leads to a decrease in shale porosity and hence shale permeability. Furthermore, the decrease in shale permeability is greatest near the sand/shale interface. This implies that the shale-water influx would be smaller in the present case than that in the constant property case solved by the semi-analytical method. For the low compressibility case (Case 4), the gas production rate fell below the minimum rate at $t \sim 23.5$ years. In the high compressibility case, the well was producing in excess of the minimum production rate at $t = 30$ years. The brine and gas production rates at the latter time are 8180 STB/D and 173,600 SCF/D respectively.

III. SUMMARY AND CONCLUSIONS

The main purpose of this report is to assess energy recovery from relatively large-volume geopressured reservoirs using data from the DOE well-testing program. Since the available data on reservoir volume and formation compressibility were insufficient, it was decided to conduct this study in two parts. In this first part of the study, the Pleasant Bayou reservoir was adopted as the base case, and the various important formation, fluid and well parameters were varied around their base values to investigate their impact on brine and gas recovery. The second part of this study will be concerned with fluid production from specific geopressured reservoirs and will be described in a future report.

The specific parameters investigated in this series of calculations were formation permeability, pore-fluid salinity, temperature and gas content, well radius and location with respect to boundaries, desired maximum (i.e., initial) flow rate, and possible shale recharge. The results of these calculations can be summarized as follows:

1. Total fluid (brine and gas) production depends strongly upon formation permeability. This is due to the fact that a well must be abandoned when the flow rate becomes too small to be economic. In low permeability reservoirs, the latter point will be reached sooner than in high permeability reservoirs.

2. Produced gas-water ratio (GWR) will be lower than the saturation GWR, as long as the free gas volume fraction (S_g) in the reservoir is substantially lower than the residual gas saturation (S_{gr}). For S_g equal to or greater than S_{gr}, the produced GWR can vastly exceed the saturation value. Furthermore, the presence of free

gas will tend to provide pressure support and thus lead to greater (as compared to no free gas case) fluid recovery.

3. The amount of fluid (brine and/or gas) recovered as a fraction of the resource in situ is nearly independent of pore-fluid salinity and temperature. The in situ gas content and the cumulative volume of gas produced are, of course, profoundly influenced by the pore-fluid salinity and temperature.

4. In the present case, because of the relatively large formation permeability employed, well radius and drainage shape (i.e., location of well vis a vis boundaries) were found to have little influence on long-term production behavior. The importance of these parameters will, however, increase with a decrease in formation permeability.

5. Efficient generation of electric power from geopressured brine requires that the brine be supplied at a nearly constant rate to the power plant. This implies that the brine be produced at a rate (essentially constant) lower than that (usually variable) necessary to recover gas in the shortest possible time. The increase in operating costs resulting from the necessity to continue production operations over a longer period of time may, however, make the latter (i.e., production at a constant rate) uneconomic.

6. For vertical shale permeabilities which are at least of the order of 10^{-5} md, shale recharge will constitute an important reservoir drive mechanism and will result in a much larger fluid recovery than that possible in the absence of shale dewatering.

REFERENCES

Alexander, J. H., S. K. Garg, J. W. Pritchett and J. H. Weare, "Development of a Physicochemical Model for Geopressured Brine Reinjection," S-CUBED, La Jolla, California, Report No. R-82-5195, December 1981.

Bebout, D. G., R. G. Loucks, and A. R. Gregory," Geological Aspects of Pleasant Bayou Geopressured Geothermal Test Well, Austin Bayou Prospect, Brazoria County, Texas," in Proceedings Fourth United States Gulf Coast Geopressured - Geothermal Energy Conference: Research and Development, (Eds. M. H. Dorfman and W. L. Fisher), Center for Energy Studies, the University of Texas at Austin, Austin, Texas, Vol. 1, pp. 11-45, 1979.

Boulton, N.S., "Analysis of Data from Non-Equilibrium Pumping Tests Allowing for Delayed Yield from Storage," Proceedings of Institute for Civil Engineers, London, England, Vol. 26, pp. 469-82, 1963.

Boulton, N.S. and T.D. Streltsova, "New Equations for Determining the Formation Constants of an Aquifer from Pumping Test Data," Water Resources Research, Vol. 11, No. 1, pp. 148-53, 1975.

Boulton, N.S. and T.D. Streltsova, "Unsteady Flow to a Well in a Two-Layered Water-Bearing Formation," Journal of Hydrology, Vol. 35, pp. 245-56, 1977.

Doscher, T. M., M. Azari, and I. Ershaghi, "Numerical Simulation of the Effect of Critical Gas Saturation and Other Parameters on the Productivity of Methane from Geopressured Aquifers," Journal of Petroleum Technology, Vol. 34, pp. 1880-1886, August 1982.

Gambolati, G., "Transient Free Surface Flow to a Well: An Analysis of Theoretical Solutions," Water Resources Research Vol. 12, No. 1, pp. 27-39, 1976.

Garg, S. K., J. W. Pritchett, D. H. Brownell, Jr., and T. D. Riney, "Geopressured Geothermal Reservoir and Wellbore Simulation," S-CUBED, La Jolla, California, Report No. SSS-R-78-3639, 1978.

Garg, S. K., J. W. Pritchett, L. F. Rice, and T. D. Riney, "Well Test Analysis and Reservoir Predictions for Geopressured Geothermal Systems (1979-1980)," S-CUBED, La Jolla, California, Report No. DOE/ET/27202-3, September 1980.

Garg, S. K., T. D. Riney, and J. M. Fwu, "Analysis of Phase 1 Flow Data from Pleasant Bayou No. 2 Geopressured Well," S-CUBED, La Jolla, California, Report No. DOE/NV10150-1, March 1981.

Garg, S.K., T.D. Riney, and J.M. Fwu, "Analysis of Phase 1 Flow Data from Pleasant Bayou No. 2 Geopressured Well," S-CUBED, La Jolla, California, Report No. DOE/NV/10150-1, March 1981.

Hantush, M.S., "Modification of the Theory of Leaky Aquifers," Journal of Geophysical Research, Vol. 65, No. 11, pp.3713-25, 1960.

Hantush, M.S., "Hydraulics of Wells," Advances in Hydroscience, V.T. Chow (ed.) Academic Press Inc., New York City pp. 281-432, 1964.

Hawkins, M. F., Jr., "Investigations on the Geopressured Energy Resource of Southern Louisiana," Petroleum Engineering Department, Louisiana State University, Baton Rouge, Louisiana, Report No. ORO-4889-14, 1977.

Hise, B. R., "Natural Gas from Geopressured Zone," in Natural Gas from Unconventional Geologic Sources, The National Research Council, Board of Mineral Resources, Commission on Natural Resources, National Academy of Sciences, pp. 41-63, 1976.

Javandel, T. and P.A. Witherspoon, "Analytical Solution of a Partially Penetrating Well in a Two-Layer Aquifer," Water Resources Research, Vol. 19, No. 2, pp. 567-78, 1983.

Jones, P. H., "Natural Gas Resources of the Geopressured Zones in the Northern Gulf of Mexico Basin," in Natural Gas from Unconventional Geologic Sources, The National Research Council, Board of Mineral Resources, Commission on Natural Resources, National Academy of Sciences, pp. 17-33, 1976.

Kuuskraa, V. A., J. P. Brashear, T. M. Doscher, and L. E. Elkins, "Vast Potential Held by Four Unconventional Gas Sources," Oil and Gas Journal, Vol. 77, No. 24, pp. 47-54, June 12, 1978.

Loucks, R. G., D. L. Richmann, and K. L. Milliken," Factors Controlling Porosity and Permeability in Geopressured Frio Sandstone Reservoirs, General Crude Oil/Department of Energy Pleasant Bayou Test Wells, Brazoria County, Texas," in Proceedings Fourth United States Gulf Coast Geopressured - Geothermal Energy Conference: Research and Department (Eds. M. H. Dorfman and W. L. Fisher), Center for Energy Studies, the University of Texas at Austin, Austin, Texas, Vol. 1, pp. 46-84, 1979.

Martin, J. C., "A Study of Simultaneous Production of Water and Gas from Aquifers Containing Initial Immobile Free Gas," Society of Petroleum Engineers Paper No. 8356, 1979.

Matthews, C. S., F. Brons, and P. Hazebroek," A Method for Determination of Average Pressure in a Bounded Reservoir," Transactions AIME, Vol. 201, pp. 182-191, 1954.

Muffler, L. J. P. and R. Cataldi, "Methods for Regional Assessment of Geothermal Resources," Geothermics, Vol. 7, No. 2-4, pp. 53-89, 1978.

National Petroleum Council, "Geopressured Brines," Vol. IV in Unconventional Gas Sources, June 1980.

Neuman, S.P. and P.A. Witherspoon, "Theory of Flow in a Confined Two-Aquifer System," Water Resources Research, Vol. 5, No.4, pp. 803-16, 1969.

Neuman, S.P., "Effect of Partial Penetration on Flow in Unconfined Aquifers Considering Delayed Gravity Response," Water Resources Research, Vol. 10, No.2, pp. 303-12, 1974.

Papadopulos, S. S., R. H. Wallace, Jr., J. B. Wesselman and R. E. Taylor," Assessment of Onshore Geopressured - Geothermal Resources in the Northern Gulf of Mexico Basin," in Assessment of Geothermal Resources of the United States - 1975 (Eds. D. E. White and D. L. Williams), United States Geological Survey Circular No. 726, pp. 125-146, 1975.

Pritchett, J. W., S. K. Garg, M. H. Rice and T. D. Riney, "Geopressured Reservoir Simulation," S-CUBED, La Jolla, California, Report No. SSS-R-79-4022, June 1979.

Roberts, B. W., "Relative Permeability Measurements of Texas Gulf Coast Sandstones at Low free Gas Saturations," Center for Earth Sciences and Engineering - Division for Rock Mechanics, the University of Texas at Austin, Austin, Texas, Report No. UT 80-2, 1980.

Stehfest, H., "Algorithm 368-Numerical Inversion of Laplace Transforms," D-5, Communications ACM (Jan. 1970) Vol. 13, No. 1, pp. 47-49, January, 1970.

Streltsova, T.D., "Buildup Analysis - for Interference Tests in Stratified Formations," Journal of Petroleum Technology, Vol. 36, pp. 301-10, February, 1984.

Swanson, R. K., "Geopressured Energy Availability," Southwest Research Institute, San Antonio, Texas, Final Report for Research Project 1272-1, July 1980.

Wallace, R. H., Jr., T. F. Kraemer, R. E. Taylor and J. B. Wesselman, "Assessment of Geopressured - Geothermal Resources in the Northern Gulf of Mexico Basin," in Assessment of Geothermal Resources of the United States - 1978 (Ed. L. J. P. Muffler), United States Geological Survey Circular No. 790, pp. 132-155, 1979.

Wallace, W. E., "Water Production from Abnormally Pressured Gas Reservoirs in South Louisiana, Part II," Society of Petroleum Engineers Paper No. 2225, 1968.

Westhusing, K., "Department of Energy Geopressured Geothermal Program," in Proceedings Fifth Conference on Geopressured Geothermal Energy (Eds. D. G. Bebout and A. L. Bachman), Louisiana State University, Baton Rouge, Louisiana, pp. 3-6, 1981.

APPENDIX

"A Semi-Analytical Approach to Analyzing
Recovery of Brine from a Bounded Reservoir
with
Crossflow from Confining Shales"

We consider the case of a high permeability layer (sand) sandwiched between two low permeability layers (shale). A well is considered to penetrate the sand and shale layers but to be perforated only in the sand layer (Figure A-1). As the well is produced, the flow in the sand layer will be augmented by induced flow from the overlying and underlying shale layers. Hantush (1964) has provided a transient flow analysis of the response of such a layered reservoir in which the interlayer crossflow is taken into account. His analysis is restricted to reservoirs of infinite lateral extent and is based on the assumptions that the sand/shale parameters are constant, the flow in the shale is vertical, and the flow in the sand may be treated as horizontal and radial. These assumptions have been used extensively in the hydrogeology literature in developing methods of analyzing the effects of crossflow when interpreting pressure data from well tests of limited duration. Analytic solutions for other systems of infinite lateral extent have been presented for leaky aquifers (Hantush 1960 and 1964), confined two-aquifer systems (Neuman and Witherspoon, 1969), unconfined flows (Boulton 1963, Gambolati 1976, Neuman 1974) and aquifer-aquitard systems (Boulton and Streltsova 1975 and 1977; Javandel and Witherspoon, 1983).

Recently, the extent of pressure support due to crossflow from formations adjacent to an oil bearing sand has been examined by Streltsova (1983). She has presented type curves that take into account the interlayered crossflow and applied them to analyze pressure buildup data from interference tests at a water injectivity test site near Prudhoe Bay, Alaska. Her results are also restricted, however, to systems of infinite lateral extent.

In the present case, we are interested in the production of geopressured-geothermal fluids from geopressured strata comprised of sequences of undercompacted sandstones and shales. The interstitial brines are hot and appear to be saturated with dissolved methane. In assessing what fraction of the resource base may be recovered, it is required to evaluate the effect of fluid influx from adjacent

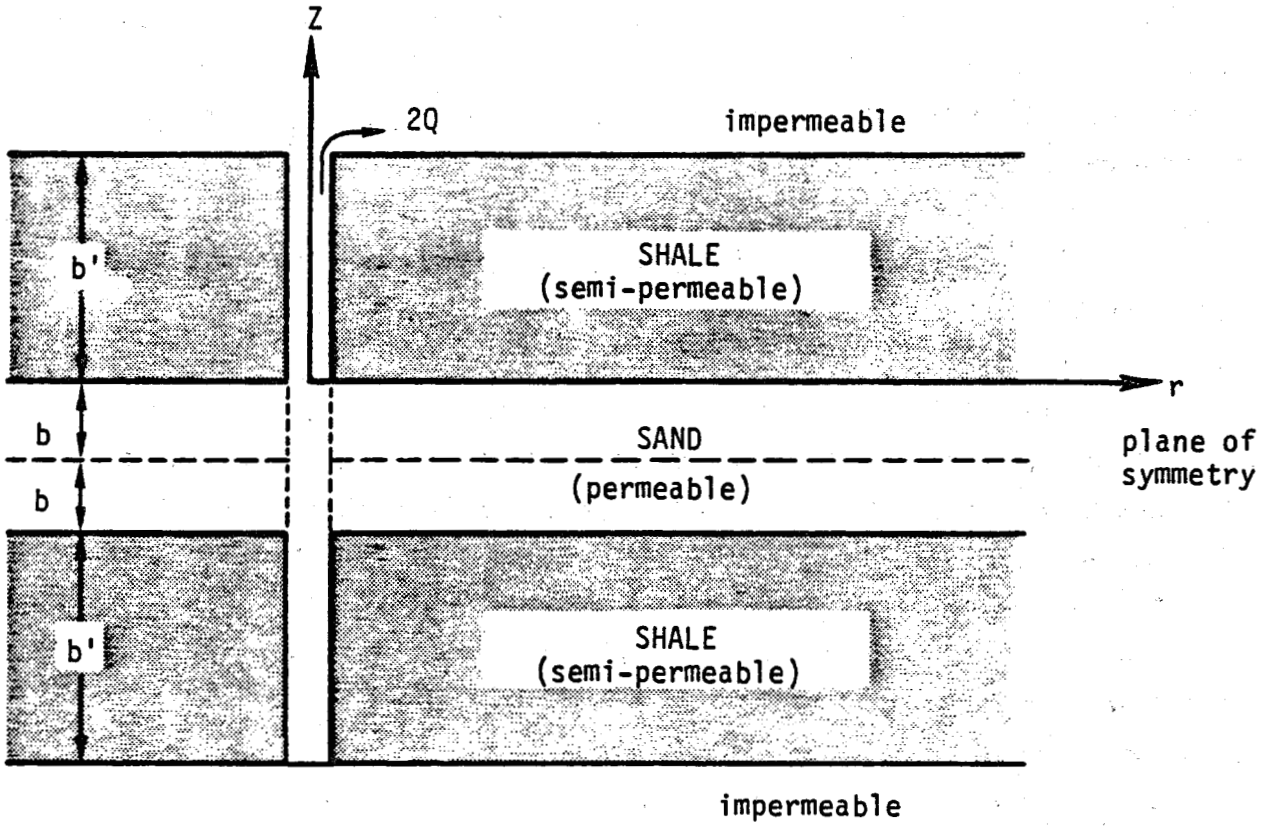

(a)

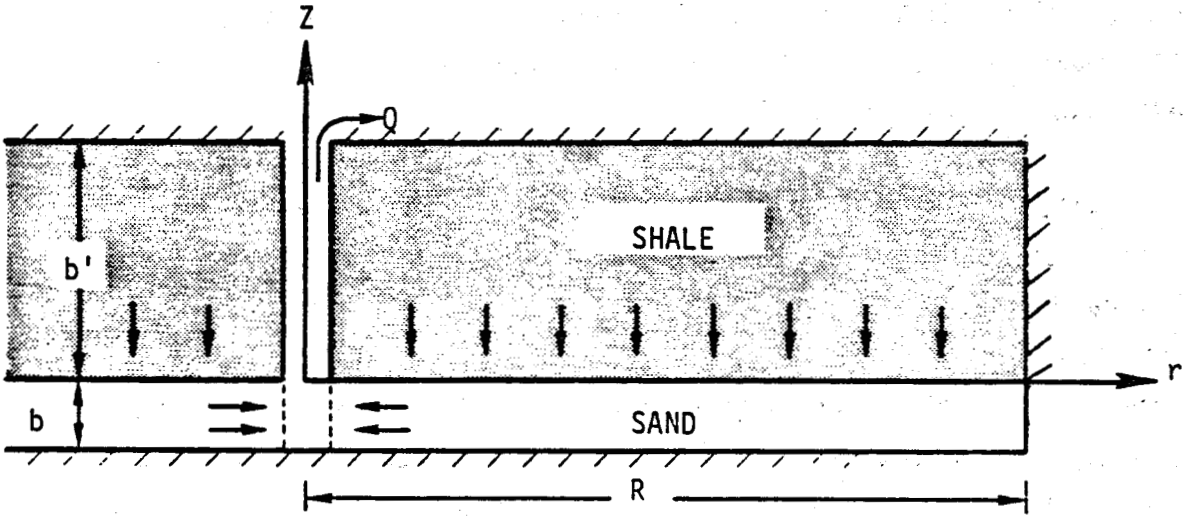

(b)

Figure A-1. Producing Layer Sandwiched between Semi-Permeable Layers

shale layers into a producing sandstone layer. Interest, therefore,includes analysis of the long-term effect (depletion behavior) of interlayered crossflow in addition to interpretation of short-term pressure drawdown/buildup tests of wells completed in geopressured-geothermal sands.

Depletion behavior of a geopressured sand/shale system bounded laterally by sealing faults may be analyzed by solution of the leaky aquifer equations for the case of a closed cylindrical reservoir of radius R. By symmetry, we need only consider the half of the sand/shale configuration (Figure A-1b) which lies above the plane of symmetry. If we assume the well to be producing fluid at a constant volume rate (Q from each symmetric portion) and use the hydrogeology notation employed by Hantush (1964), the governing equations for the change in hydraulic head in the shale, s_1 (r,z,t), and sand, s (r,t), layers are as follows:

SHALE:

$$\frac{\partial^2 s_1}{\partial z^2} = \frac{1}{\nu'} \frac{\partial s_1}{\partial t} \qquad \text{(A-1)}$$

$$s_1 (r,z,t) = 0 \qquad \text{(A-2)}$$

$$s_1 (r,0,t) = s (r,t) \qquad \text{(A-3)}$$

$$\frac{\partial s_1 (r,b',t)}{\partial z} = 0 \qquad \text{(A-4)}$$

SAND:

$$\frac{\partial^2 s}{\partial r^2} + \frac{1}{r} \frac{\partial s}{\partial r} + \frac{K'}{T} \frac{\partial s_1(r,0,t)}{\partial z} = \frac{1}{\nu} \frac{\partial s}{\partial t} \qquad \text{(A-5)}$$

$$s(r,0) = 0 \qquad \text{(A-6)}$$

$$\frac{\partial s(R,t)}{\partial r} = 0 \qquad \text{(A-7)}$$

$$r_w \frac{\partial s(r_w,t)}{\partial r} = - \frac{Q}{2\pi T} \qquad \text{(A-8)}$$

Here the parameter ν (ν') is given by the ratio T/S (T'/S'). The no-flow boundary condition at r = R, Equation (A-7), is the only change from the system of equations presented by Hantush (1964). The change in pressure, ΔP, and the pressure, P, in the sand (more commonly used in the petroleum literature), are related to the change in head by

$$\Delta P = \gamma s(r,t) \qquad \text{(A-9)}$$

$$P = P_i - \Delta P \qquad \text{(A-10)}$$

Here P_i denotes the initial reservoir pressure.

If the Laplace transformation is applied to the shale equations, a general solution to Equation (A-1) can be readily obtained. The particular solution satisfying Equations (A-2), (A-3) and (A-4) in Laplace space is

$$\bar{s}_1 = \bar{s} \left[\frac{\cosh (b'-z)\sqrt{p/\nu'}}{\cosh b' \sqrt{p/\nu'}} \right] \qquad \text{(A-11)}$$

Here p is the Laplace parameter and $\bar{s}_1(r,z,p)$ and $\bar{s}(r,p)$ are the Laplace transforms of $s_1(r,z,t)$ and $s(r,t)$, respectively.

Application of the Laplace transform to the sand equations yields

$$\frac{\partial^2 \bar{s}}{\partial r^2} + \frac{1}{r} \frac{\partial \bar{s}}{\partial r} - \lambda^2 \bar{s} = 0 \qquad \text{(A-12)}$$

$$\frac{\partial \bar{s}}{\partial r} (R,p) = 0 \qquad \text{(A-13)}$$

$$r_w \frac{\partial \bar{s}\ (r_w,p)}{\partial r} = - \frac{Q}{2\pi T} \frac{1}{p} \qquad \text{(A-14)}$$

with λ_1 defined by

$$\lambda_1^2 = \frac{p}{\nu} + \frac{K'}{b't} \left(b'\sqrt{p/\nu'}\right) \tanh \left(b'\sqrt{p/\nu'}\right) \qquad \text{(A-15)}$$

Here we have used Equation (A-11) to express the crossflow term in Equation (A-12) in terms of $\bar{s}$ rather than $\bar{s}_1$. The general solution in Laplace space of Equation (A-12) is

$$\bar{s}\ (r,p) = \frac{Q}{2\pi T} \left\{ D_1\ K_o\ (\lambda_1 r) + D_2\ I_o\ (\lambda_1 r) \right\} \qquad \text{(A-16)}$$

The particular solution satisfying Equations (A-13) and (A-14) is obtained by setting

$$D_1 = D_2\ \frac{I_1\ (\lambda_1 R)}{K_1\ (\lambda_1 R)} \qquad \text{(A-17)}$$

$$D_2 = \frac{-1}{r_w\ \lambda_1\ p} \left[I_1(\lambda_1 r_w) - \frac{I_1(\lambda_1 R)}{K_1(\lambda_1 R)}\ K_1(\lambda_1 r_w) \right]^{-1} \qquad \text{(A-18)}$$

For $R = \infty$, Hantush (1964) derived asymptotic expressions for $s\ (r,t)$ at large and small values of time from the behavior of $\bar{s}\ (r,p)$ for small and large values of the transform parameter p. The methods do not readily apply for R finite. Furthermore, Equation (16) is the most convenient form to calculate the changes in head (and pressure) by applying the numerical Laplace inversion presented by Stehfest (1970). Even for the special case of $R = \infty$, the latter method requires less computing time than the asymptotic expressions of Hantush and provides solutions for all values of t.

From the definition of the storage coefficient (S), the rate of fluid production from the sand half-layer (q_s) is given by

$$r_w \frac{\partial q_s}{\partial r} = 2\pi r\ S \frac{\partial s}{\partial t} \qquad \text{(A-19)}$$

Or, in Laplace space,

$$\bar{q}_s = \frac{2\pi S}{r_w} \int_0^R L\left\{\frac{\partial s}{\partial t}\right\} r \, dr$$

Use of Equation (A-6) yields

$$\bar{q}_s = \frac{2\pi Sp}{r_w} \int_0^R \bar{s} \, r \, dr \qquad \text{(A-20)}$$

To illustrate the effect of fluid influx from semi-permeable shale layers above and below a producing geopressured-geothermal sandstone, we have performed the numerical Laplace inversion*

$$\Delta P = \gamma \, s(r,t) \qquad \text{(A-21)}$$

$$= \frac{\gamma Q}{2\pi T} L^{-1} \left\{ D_1 K_o(\lambda_1 r) + D_2 I_o(\lambda_1 r) \right\}$$

for input parameters adopted from the Pleasant Bayou reservoir data base. The following data are derived from the U.S. Department of Energy tests on the Pleasant Bayou No. 2 Well, Brazori County, Texas (Garg, et al, 1981).

FLUID:

Compressibility, $C_f = 4.35 \times 10^{-10}$ Pa^{-1} (3×10^{-6} psi^{-1})
Viscosity, $\mu = 2.7 \times 10^{-4}$ Pa-s (0.27 cp)
Specific Weight, $\gamma = \rho g = 10.417 \times 10^{3}$ kg/m^{2}s

SAND:

Half-thickness, b = 9.144 m (h = 2b = 60 ft)
Porosity, $\phi = 0.18$
Total Compressibility, $C_T = 10.962 \times 10^{-10}$ Pa^{-1} (7.56×10^{-6} psi^{-1})

---

*A program for performing the numerical Laplace inversion based on the method of Stehfest (1970) has been written by Dr. D.H. Brownell at S-CUBED. It was used for all calculations presented in this report.

Storage, $S = b\gamma\phi C_T = 1.8795 \times 10^{-5}$

Permeability, $k_h = 1.875 \times 10^{-13}$ m^2 (190 md)

Conductivity, $K = \gamma k_h/\mu = 7.234 \times 10^{-6}$ m/s

Transmissivity, $T = b\gamma k_h/\mu = 6.615 \times 10^{-5}$ m^2/s

SHALE:

Thickness, $b' = 18.288$m (60 ft)

Porosity, $\phi' = 0.18$

Total Compressibility, C_T'

Storage, $S' = b' \gamma\phi' C_T'$

Permeability, k_v'

Conductivity, $K' = \gamma k_v' /\mu$

Transmissivity, $T' = b' \gamma k_v' C_T'$

} See Table A-1

The values of the matrix compressibility (C_m') and vertical permeability (k_h') in the shale can only be estimated. Table A-1 presents ranges of values which include plausible values of these parameters. The corresponding values of

$$C_T' = C_f + \frac{1-\phi'}{\phi'} C_m' \quad , \qquad \text{(A-22)}$$

K', S' and $\nu' = T'/S' = K'b'/S'$ are also listed in Table A-1.

The initial pressure in the Pleasant Bayou reservoir was

$$P_i = 7.7 \times 10^7 \text{ Pa (11,168 psi).}$$

The volume of the sand layer, thickness $h = 2b = 18.288$ m (60 ft), is assumed to be $V = 17.126 \times 10^8$ m^3 (6.048×10^{10}ft^3). The depletion behavior of the reservoir can be investigated under the assumption that the Pleasant Bayou No. 2 well is located at the center of a closed cylindrical reservoir with radius

$$R = \sqrt{\frac{V}{\pi h}} = \sqrt{\frac{17.126 \times 10^8}{\pi\ 18.288}} = 5460\text{m}$$

Table A-1

Values of Formation Parameters for Semi-Permeable Shale Layer

Case No.	k'_v (md)	C'_m (psi^{-1})	C'_T (Pa^{-1})	S'	K' (m/s)	υ' (m^2/s)
1	0	–	–	–	0	0
2	10^{-5}	10^{-5}	7.047×10^{-9}	2.416×10^{-4}	3.81×10^{-13}	2.883×10^{-8}
3	10^{-4}	10^{-5}	7.047×10^{-9}	2.416×10^{-4}	3.81×10^{-12}	2.883×10^{-7}
4	10^{-5}	10^{-4}	6.657×10^{-9}	2.283×10^{-3}	3.81×10^{-13}	3.052×10^{-9}
5	10^{-4}	10^{-4}	6.657×10^{-9}	2.283×10^{-3}	3.81×10^{-12}	3.052×10^{-8}
6	10^{-3}	10^{-4}	6.657×10^{-9}	2.283×10^{-3}	3.81×10^{-11}	3.052×10^{-7}
7	10^{-3}	10^{-5}	7.047×10^{-9}	2.416×10^{-4}	3.81×10^{-11}	2.883×10^{-6}

The well is assumed to be flowing at the constant rate of 2Q = 40,000 bbl/D, or Q = 20,000 bbl/D for each half of the sand/shale configuration (Figure 1b). The equivalent bottomhole flow rate is

$$Q = 0.0368 \text{ m}^3/\text{s}$$

The constant flow rate is assumed to be maintained until the bottomhole pressure drops to the hydrostatic value of 7,250 psi.

Figure A-2 shows the bottomhole drawdown pressure at the sandface ($r = r_w$) computed from the Laplace inversion of Equation (A-16) and the use of Equations (A-9) and (A-10). Results are shown for each of its seven choices for the shale parameters k_v' and C_m' (Table A-1). The remaining sand/shale parameters, reservoir dimensions and well operation parameters were fixed as described above.

For the case of no crossflow from the shale layers (Case No. 1), the flow quickly attains semi-steady state and the pressure thereafter decreases linearly to the cutoff value of 7,250 psi in about 2.5 years. With crossflow effects included, the well continues to flow at the constant rate of 2Q = 40,000 bbl/D for times far beyond 2.5 years.

The results for Cases 2, 3 and 7 illustrate the effect of changing shale vertical permeability ($k_v' = 10^{-5}$, 10^{-4} and 10^{-3} md respectively) for shale matrix compressibility fixed at $C_m' = 10^{-5}$ psi^{-1}. The results for Cases 4, 5 and 6 illustrate the same effect for $C_m' = 10^{-4}$ psi^{-1}. The pressure support provided by the crossflow from the shale dewatering permits the well to continue to operate at 40,000 bbl/D for approximately 6 years even with the most conservative parameter assumptions employed (Case 2).

The results for Cases 2 and 4 illustrate the effect changing

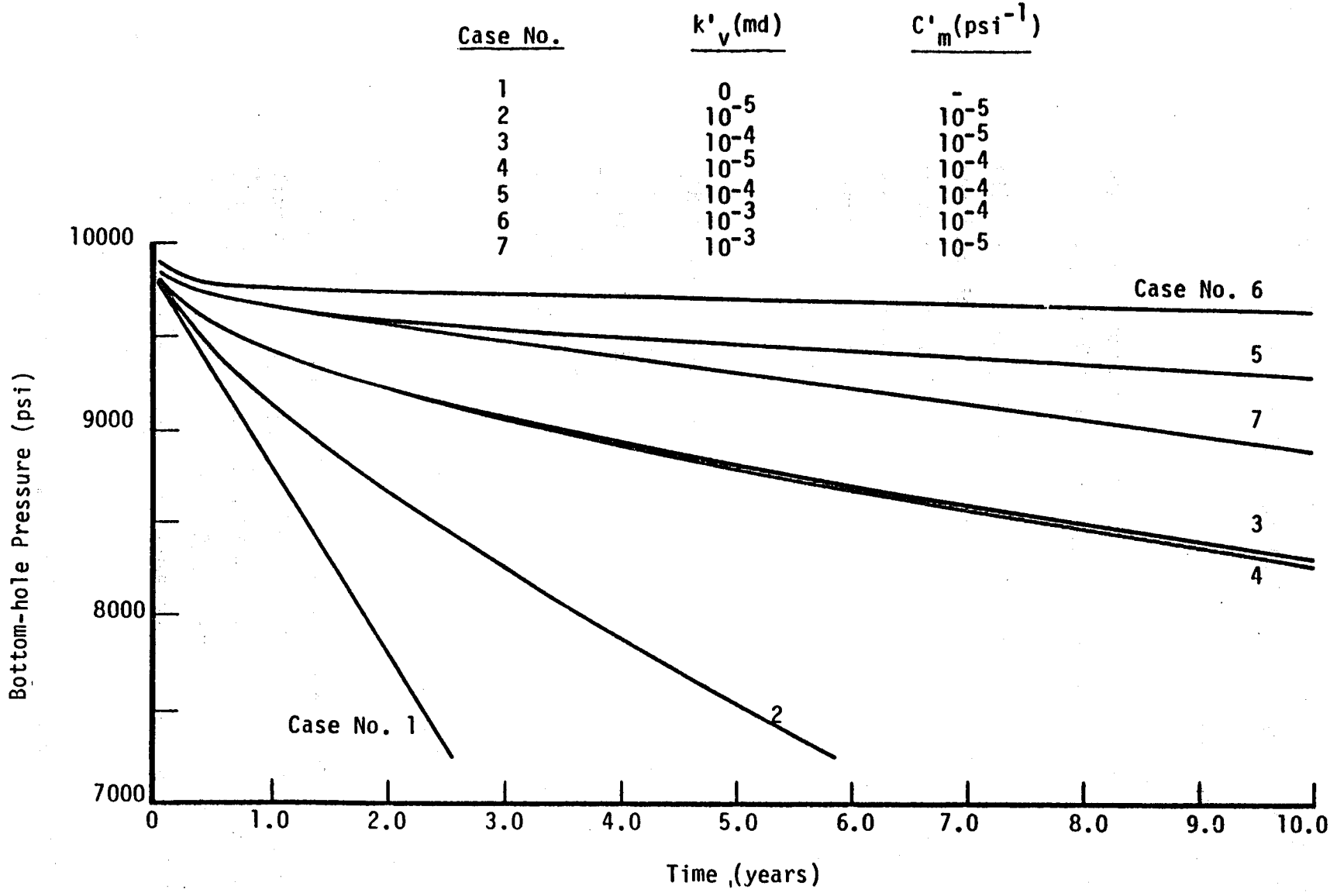

Figure A-2. Sensitivity of Bottom-hole Pressure to Vertical Permeability and Compressibility of the Shale (Finite Reservoir)

the shale matrix compressibility ($C_m' = 10^{-5}$ and 10^{-4} psi^{-1} respectively) for $k_v' = 10^{-5}$ md. The results for Cases 3 and 5 (Cases 6 and 7) illustrate the same effect for $k_v' = 10^{-4}$ md ($k_v' = 10^{-3}$ md). From Cases 3 and 4 we see that a ten-fold increase in k_v' has essentially the same effect as a ten-fold increase C_m'.

For illustrative purposes Laplace inversion calculations were also performed for the case of a reservoir of infinite lateral extent ($R = \infty$). The results for the seven choices for the shale parameters k_v' and C_m' employed in the calculations (Table A-1) are shown in Figure A-3. The calculations for the infinite reservoir were also performed using the asymptotic expressions presented by Hantush (1964) for this particular case. The results were essentially identical but the Laplace inversion required only a fraction of the computing time required for the asymptotic expressions. The asymptotic expression for the fraction of fluid production which comes from the sand (presented by Hantush, 1964),

$$\frac{(2'q_s)}{(2Q)} = \exp(nt)\ \mathrm{erfc}\ (\sqrt{nt}) \qquad \text{(A-23)}$$

$$n = \frac{K'S'}{b'S^2}\ ,\ t < \frac{b'S'}{10K'} \qquad \text{(A-24)}$$

is useful for this special case. The results for the seven cases are shown in Figure A-4. Similar results for R finite could be obtained by Laplace inversion of Equation (A-20).

For completeness, we also present the Horner plots of the drawdown and buildup response for the seven cases listed in Table A-1. The buildup responses shown in Figure A-5 are for a well subsequent to production for $t_p = 10^6$s (no boundary effects present). It is of interest to note that analysis which ignores crossflow would imply incorrect values for the sand permeability and the well's skin. Type curves for drawdown/buildup in an infinite reservoir have been presented by Streltsova (1984).

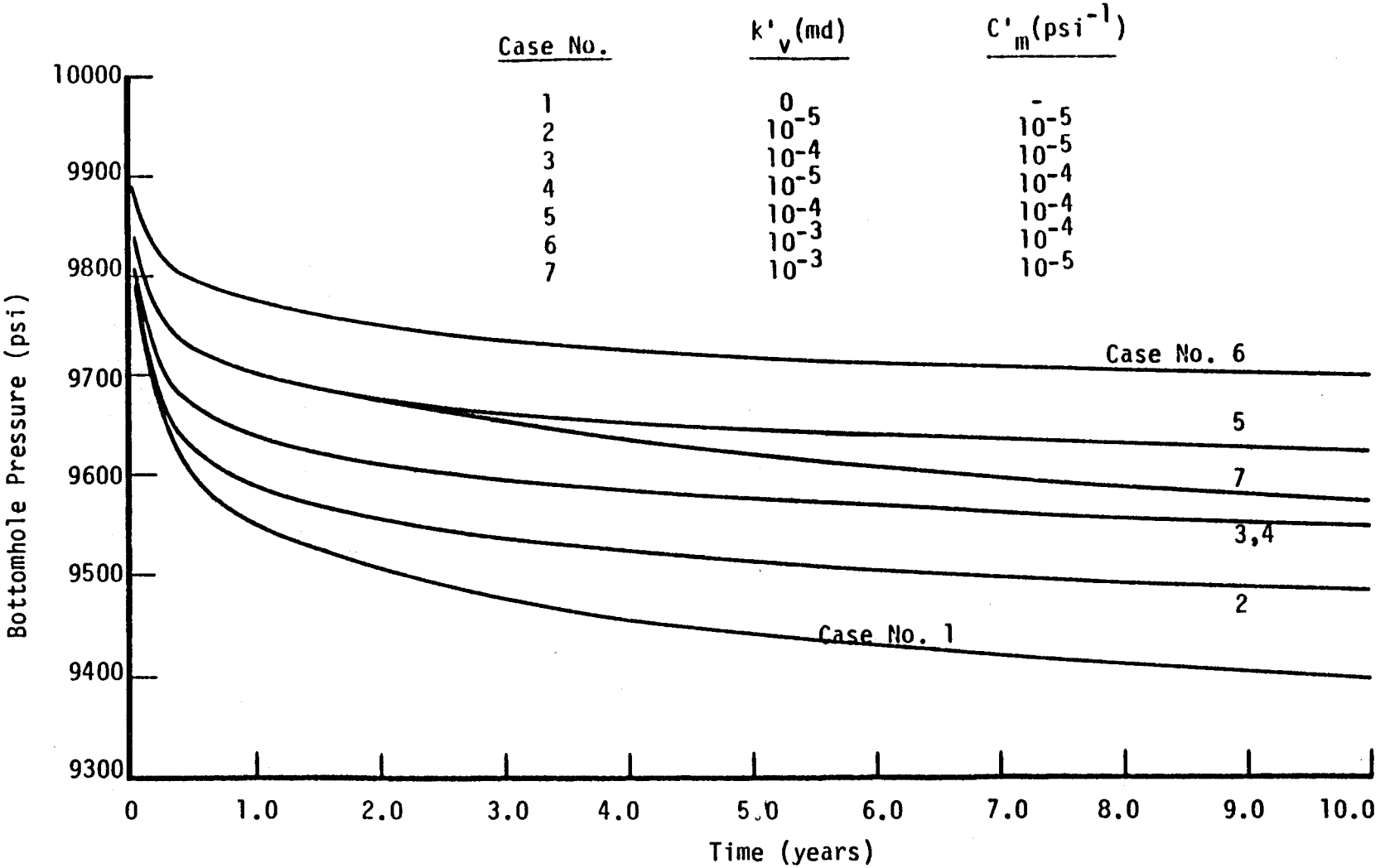

Figure A-3. Sensitivity of Bottomhole Pressure to Vertical Permeability and Matrix Compressibility of the Shale (Infinite Reservoir)

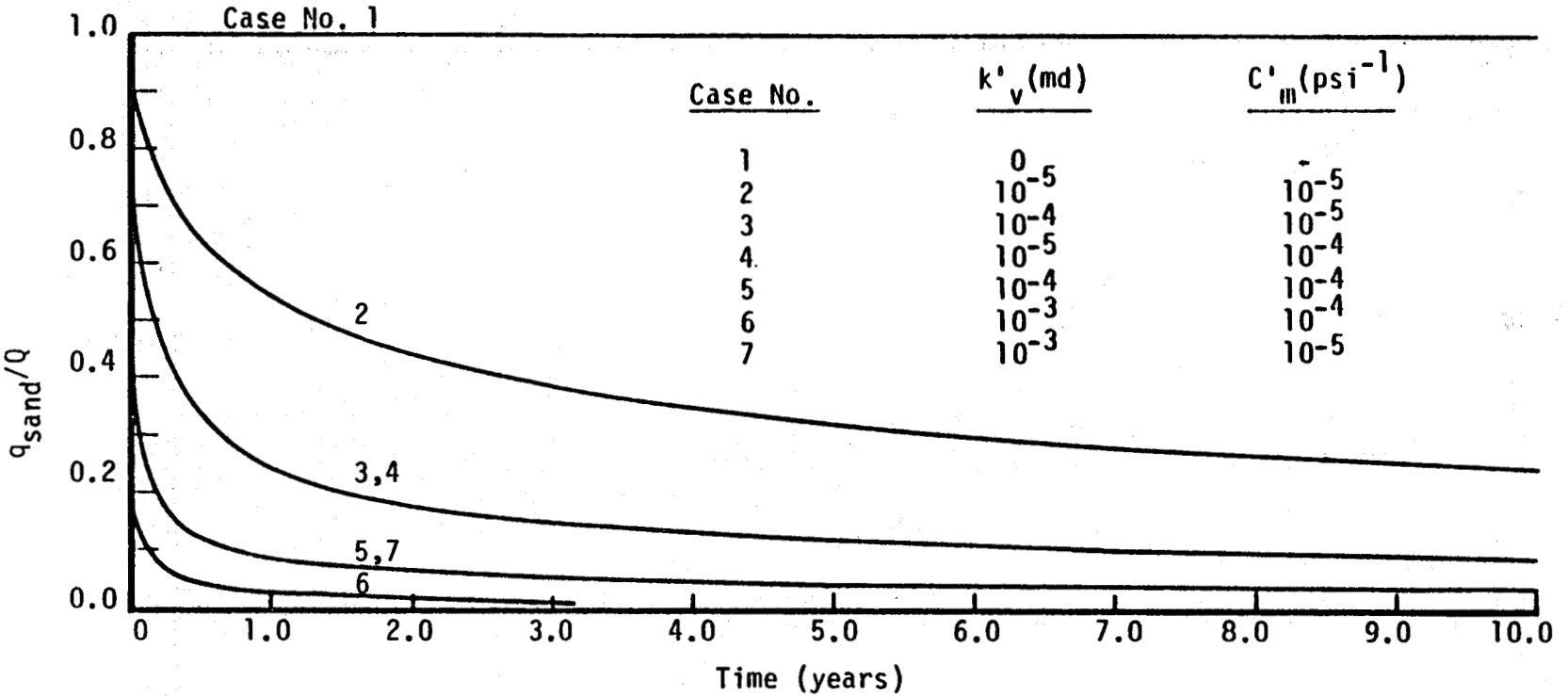

Figure A-4. Fraction of Fluid Produced from Sand Layer

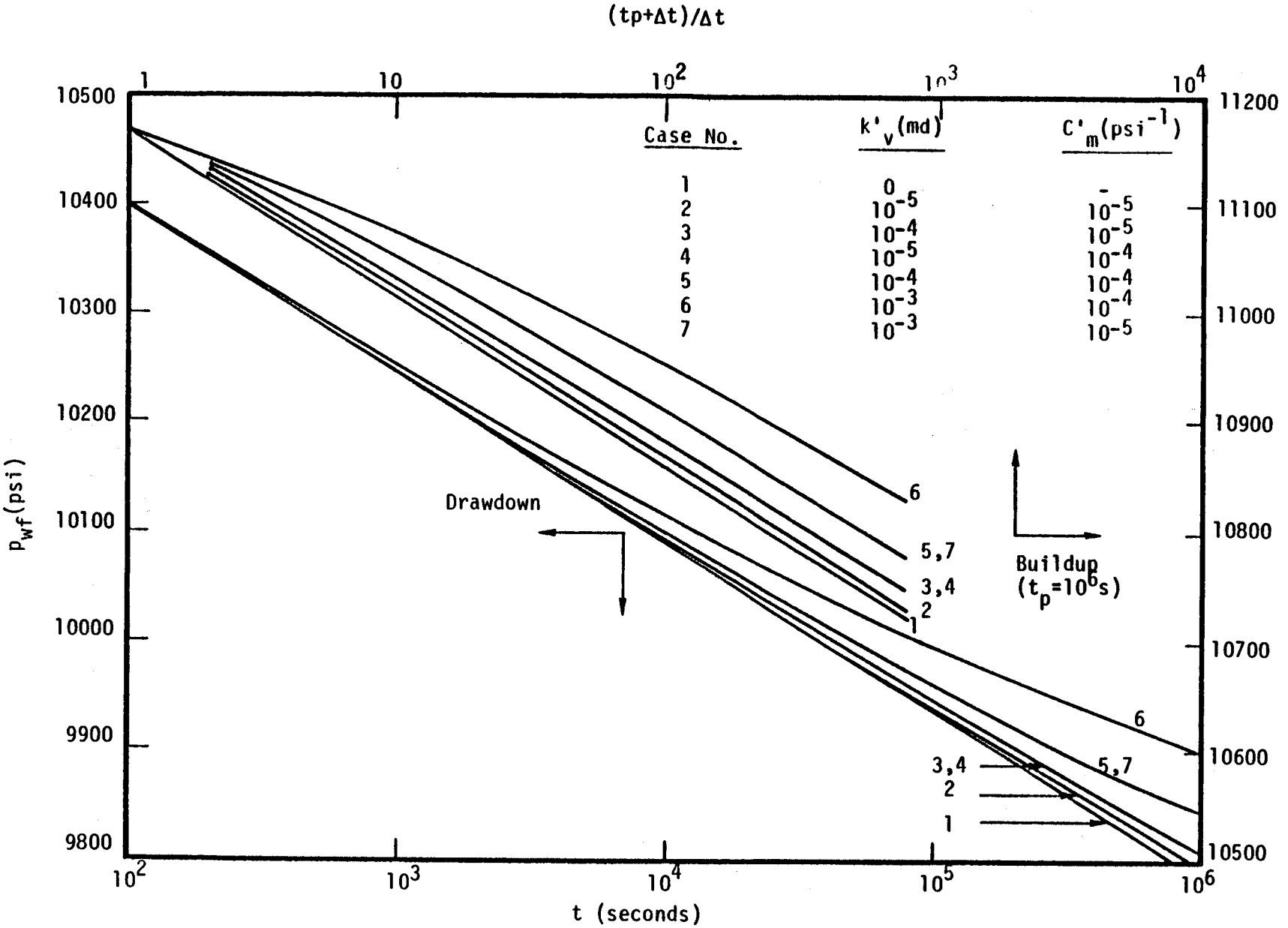

Figure A-5 Sensitivity of Drawdown/Buildup Response to Shale Parameters